recessive mutations in the cardiac sodium channel gene (SCN5A). *J Clin Invest*. 2003;112:1019–1028.
8. Smits JP, Koopmann TT, Wilders R, Veldkamp MW, Opthof T, Bhuiyan ZA, Mannens MM, Balser JR, Tan HL, Bezzina CR, Wilde AA. A mutation in the human cardiac sodium channel (E161K) contributes to sick sinus syndrome, conduction disease and Brugada syndrome in two families. *J Mol Cell Cardiol*. 2005;38:969–981.
9. Veldkamp MW, Wilders R, Baartscheer A, Zegers JG, Bezzina CR, Wilde AA. Contribution of sodium channel mutations to bradycardia and sinus node dysfunction in LQT3 families. *Circ Res*. 2003;92:976–983.
10. Makita N, Sasaki K, Groenewegen WA, Yokota T, Yokoshiki H, Murakami T, Tsutsui H. Congenital atrial standstill associated with coinheritance of a novel SCN5A mutation and connexin 40 polymorphisms. *Heart Rhythm*. 2005;2:1128–1134.
11. Makiyama T, Akao M, Tsuji K, Doi T, Ohno S, Takenaka K, Kobori A, Ninomiya T, Yoshida H, Takano M, Makita N, Yanagisawa F, Higashi Y, Takeyama Y, Kita T, Horie M. High risk for bradyarrhythmic complications in patients with Brugada syndrome caused by SCN5A gene mutations. *J Am Coll Cardiol*. 2005;46:2100–2106.
12. Schulze-Bahr E, Neu A, Friederich P, Kaupp UB, Breithardt G, Pongs O, Isbrandt D. Pacemaker channel dysfunction in a patient with sinus node disease. *J Clin Invest*. 2003;111:1537–1545.
13. Mohler PJ, Splawski I, Napolitano C, Bottelli G, Sharpe L, Timothy K, Priori SG, Keating MT, Bennett V. A cardiac arrhythmia syndrome caused by loss of ankyrin-B function. *Proc Natl Acad Sci U S A*. 2004;101:9137–9142.
14. Holm H, Gudbjartsson DF, Sulem P, Masson G, Helgadottir HT, Zanon C, Magnusson OT, Helgason A, Saemundsdottir J, Gylfason A, Stefansdottir H, Gretarsdottir S, Matthiasson SE, Thorgeirsson GM, Jonasdottir A, Sigurdsson A, Stefansson H, Werge T, Rafnar T, Kiemeney LA, Parvez B, Muhammad R, Roden DM, Darbar D, Thorleifsson G, Walters GB, Kong A, Thorsteinsdottir U, Arnar DO, Stefansson K. A rare variant in MYH6 is associated with high risk of sick sinus syndrome. *Nat Genet*. 2011;43:316–320.
15. Dobrzynski H, Boyett MR, Anderson RH. New insights into pacemaker activity: promoting understanding of sick sinus syndrome. *Circulation*. 2007;115:1921–1932.
16. Kodama T, Serio A, Disertori M, Bronzetti G, Diegoli M, Narula N, Grasso M, Mazzola S, Arbustini E. Autosomal recessive paediatric sick sinus syndrome associated with novel compound mutations in SCN5A. *Int J Cardiol*. 2013;167:3078–3080.
17. Olgin JE, Zipes DP. Specific arrhythmias: diagnosis and treatment. In: Braunwald E, Zipes DP, Libby P, eds. *Heart Disease: A Textbook of Cardiovascular Medicine*. Philadelphia, PA: W.B. Saunders Company; 2001:815–899.
18. Schwartz PJ, Crotti L, Insolia R. Long-QT syndrome: from genetics to management. *Circ Arrhythm Electrophysiol*. 2012;5:868–877.
19. Antzelevitch C, Brugada P, Borggrefe M, Brugada J, Brugada R, Corrado D, Gussak I, LeMarec H, Nademanee K, Perez Riera AR, Shimizu W, Schulze-Bahr E, Tan H, Wilde A. Brugada syndrome: report of the second consensus conference: endorsed by the Heart Rhythm Society and the European Heart Rhythm Association. *Circulation*. 2005; 111:659–670.
20. Makita N, Behr E, Shimizu W, Horie M, Sunami A, Crotti L, Schulze-Bahr E, Fukuhara S, Mochizuki N, Makiyama T, Itoh H, Christiansen M, McKeown P, Miyamoto K, Kamakura S, Tsutsui H, Schwartz PJ, George AL Jr, Roden DM. The E1784K mutation in SCN5A is associated with mixed clinical phenotype of type 3 long QT syndrome. *J Clin Invest*. 2008;118:2219–2229.
21. Gosselin-Badaroudine P, Keller DI, Huang H, Pouliot V, Chatelier A, Osswald S, Brink M, Chahine M. A proton leak current through the cardiac sodium channel is linked to mixed arrhythmia and the dilated cardiomyopathy phenotype. *PLoS One*. 2012;7:e38331.
22. McNair WP, Ku L, Taylor MR, Fain PR, Dao D, Wolfel E, Mestroni L; Familial Cardiomyopathy Registry Research Group. SCN5A mutation associated with dilated cardiomyopathy, conduction disorder, and arrhythmia. *Circulation*. 2004;110:2163–2167.
23. Watanabe H, Yang T, Stroud DM, Lowe JS, Harris L, Atack TC, Wang DW, Hipkens SB, Leake B, Hall L, Kupershmidt S, Chopra N, Magnuson MA, Tanabe N, Knollmann BC, George AL Jr, Roden DM. Striking *In vivo* phenotype of a disease-associated human SCN5A mutation producing minimal changes *in vitro*. *Circulation*. 2011; 124:1001–1011.
24. Bennett PB, Yazawa K, Makita N, George AL Jr. Molecular mechanism for an inherited cardiac arrhythmia. *Nature*. 1995;376:683–685.
25. Chen Q, Kirsch GE, Zhang D, Brugada R, Brugada J, Brugada P, Potenza D, Moya A, Borggrefe M, Breithardt G, Ortiz-Lopez R, Wang Z, Antzelevitch C, O'Brien RE, Schulze-Bahr E, Keating MT, Towbin JA, Wang Q. Genetic basis and molecular mechanism for idiopathic ventricular fibrillation. *Nature*. 1998;392:293–296.
26. Schott JJ, Alshinawi C, Kyndt F, Probst V, Hoorntje TM, Hulsbeek M, Wilde AA, Escande D, Mannens MM, Le Marec H. Cardiac conduction defects associate with mutations in SCN5A. *Nat Genet*. 1999;23:20–21.
27. Groenewegen WA, Firouzi M, Bezzina CR, Vliex S, van Langen IM, Sandkuijl L, Smits JP, Hulsbeek M, Rook MB, Jongsma HJ, Wilde AA. A cardiac sodium channel mutation cosegregates with a rare connexin40 genotype in familial atrial standstill. *Circ Res*. 2003;92:14–22.
28. Bordachar P, Reuter S, Garrigue S, Caï X, Hocini M, Jaïs P, Haïssaguerre M, Clementy J. Incidence, clinical implications and prognosis of atrial arrhythmias in Brugada syndrome. *Eur Heart J*. 2004;25:879–884.
29. Morita H, Fukushima-Kusano K, Nagase S, Miyaji K, Hiramatsu S, Banba K, Nishii N, Watanabe A, Kakishita M, Takenaka-Morita S, Nakamura K, Saito H, Emori T, Ohe T. Sinus node function in patients with Brugada-type ECG. *Circ J*. 2004;68:473–476.

CLINICAL PERSPECTIVE

Sick sinus syndrome (SSS) is a common arrhythmia often associated with aging or organic heart diseases but may also occur in a familial form with a variable mode of inheritance. Recent studies have linked several genetic defects with familial SSS in genes including the cardiac Na channel (*SCN5A*); however, the pathogenesis and molecular epidemiology of familial SSS remain undetermined primarily because of its rarity. We genetically screened 48 members of 15 SSS families and identified 6 *SCN5A* mutations. Heterologously expressed mutant Na channels showed loss-of-function properties. Among 19 family members with *SCN5A* mutations, QT prolongation and Brugada syndrome were associated in 4 and 2 individuals, respectively. Age of onset in probands carrying *SCN5A* mutations was significantly less (12.4±4.6 years) than that in *SCN5A*-negative probands (47.0±4.6 years) or nonfamilial SSS (74.3±0.4 years). Meta-analysis of SSS probands carrying *SCN5A* mutations (n=29) indicated profound male predominance (79.3%) resembling Brugada syndrome but with a considerably earlier age of onset (20.9±3.4 years). The notable pathophysiological overlap between familial SSS and Na channelopathy indicates that familial SSS with *SCN5A* mutations may represent a subset of cardiac Na channelopathy with strong male predominance and early clinical manifestations. This study also suggests that SSS is the earliest electrophysiological manifestation of *SCN5A* mutation carriers, which may be associated with other arrhythmias such as long QT syndrome, Brugada syndrome, and dilated cardiomyopathy under the control of confounding factors including aging, hormones, other genetic variations, and undetermined environmental factors.

Journal of Arrhythmia 30 (2014) 433–438

Contents lists available at ScienceDirect

Journal of Arrhythmia

journal homepage: www.elsevier.com/locate/joa

Original Article

Spatial and transmural repolarization, and dispersion of repolarization and late potentials evaluated using signal-averaged vector-projected 187-channel high-resolution electrocardiogram in Brugada syndrome

Kimie Ohkubo, MD[a], Ichiro Watanabe, MD[a,*], Yasuo Okumura, MD[a], Masayoshi Kofune, MD[a], Koichi Nagashima, MD[a], Hiroaki Mano, MD[a], Kazumasa Sonoda, MD[a], Toshiko Nakai, MD[a], Yuji Kasamaki, MD[a], Atsushi Hirayama, MD[a], Naokata Sumitomo, MD[b], Tomohiro Nakayama, MD[c]

[a] Division of Cardiology, Department of Medicine, Nihon University School of Medicine, Tokyo, Japan
[b] Department of Pediatrics, Nihon University School of Medicine, Tokyo, Japan
[c] Department of Laboratory Medicine, Nihon University School of Medicine, Tokyo, Japan

ARTICLE INFO

Article history:
Received 23 July 2013
Received in revised form
18 October 2013
Accepted 25 October 2013
Available online 22 December 2013

Keywords:
Brugada syndrome
Recovery time
Late potential
Spatial dispersion

ABSTRACT

Background: Vector-projected 187-channel electrocardiograms (ECGs) were recorded in 45 patients with a Brugada-type ECG to evaluate spatial and transmural repolarization and dispersion of action potential duration in Brugada syndrome (BS).
Methods: Corrected recovery time (RT-c, R wave peak to the first positive maximum derivative of the T wave with Bazett correction) and RT-c dispersion were calculated. The corrected T peak-end interval (T (p-e)-c, T wave peak to the end of the T wave with Bazett correction) and T(p-e)-c dispersion were calculated.
Results: RT-c dispersion and T(p-e)-c interval were longer in patients with a type 1 ECG, but there was no significant difference in Tp-e dispersion between patients with a type 1 and those with a type 2/3 ECG. No significant correlation was noted between RT-c dispersion, T(p-e)-c dispersion, and symptoms. Late potentials ($P=0.023$) and a family history of sudden cardiac death ($P=0.0017$) were correlated with symptoms.
Conclusions: Spatial dispersion of repolarization may constitute the electrocardiographic pattern of the Brugada type ECG and conduction disturbance in addition to repolarization abnormality may contribute to the development of malignant ventricular tachyarrhythmias.

1. Introduction

Brugada syndrome (BS) is an arrhythmogenic entity characterized by the presence of ST-segment elevation in leads V1–V3 on surface electrocardiogram (ECG), the absence of structural heart disease, and a high risk of ventricular tachycardia/ventricular fibrillation (VT/VF) and sudden cardiac death (SCD) [1–3]. Risk stratification is controversial, especially in asymptomatic individuals [4–6]. Transmural dispersion of repolarization within the ventricular myocardium has been suggested to underlie arrhythmogenesis in BS [7], and ECG markers of ventricular repolarization have been reported for the identification of high-risk patients with BS [8]. We investigated whether ECG-based spatial and transmural ventricular depolarization and repolarization values are potential risk factors for arrhythmic events in BS patients. In the present study, we used the recently developed signal-averaged vector-projected 187-channel high-resolution ECG (187-channel SAVP-ECG).

2. Methods

2.1. Study patients

The study group comprised 45 consecutive patients (male/female ratio: 43/2; mean age, 51.5 ± 14.4 years) with spontaneous ($n=26$) or drug-induced (pilsicainide 1 mg/kg) ($n=19$) type 1 BS ECG phenotype. The ECG diagnosis of BS was based strictly on the recommendations of the Second Consensus Conference [3]. Structural heart disease was ruled out in all study patients by performing transthoracic echocardiography. Those with a history of syncope, documented sustained ventricular arrhythmia,

* Correspondence to: Division of Cardiology, Department of Medicine, Nihon University School of Medicine, 30-1 Oyaguchi-kamimachi, Itabashi-ku, Tokyo 173-8610, Japan. Tel.: +81 3 3972 8111; fax: +81 3 3972 1098.
E-mail address: watanabe.ichirou@nihon-u.ac.jp (I. Watanabe).

1880-4276/$ - see front matter © 2013 Japanese Heart Rhythm Society. Published by Elsevier B.V. All rights reserved.
http://dx.doi.org/10.1016/j.joa.2013.10.004

or aborted SCD were considered symptomatic. The study was approved by the Institutional Review Committee of Nihon University Hospital, and the patients signed informed consent for 187-channel SAVP-ECG recording, mutation screening for the SCN5A gene, and invasive electrophysiological study.

2.2. 187-channel SAVP ECG

187-channel SAVP-ECGs were obtained with an electrode lead system, an input box, a high-precision amplifier (HRES-1000, Fukuda Denshi Co. Ltd., Tokyo, Japan), and a personal computer. The input box generated a modified *X–Y–Z*-lead ECG, and the vector-projected 187-channel synthesized ECGs via a Mason–Likar lead system. The input signal (± 550 mV) was digitized at 2 kHz by an analog-to-digital (A/D) converter with a resolution of 0.076 μV. Ten electrodes were attached to the right shoulder, left shoulder, left lower abdomen, right lower abdomen, and the usual V1–V6 recording sites. The 187-channel SAVP-ECG recording was performed with patients in a resting position. Details of the187-channel SAVP-ECG have been reported previously [9–11]. The 187-channel SAVP-ECG variables measured in the current study are described below.

2.3. Repolarization

The RT interval was defined as the time between the peak of the R wave and the maximum positive peak of the first derivative of the T wave, which was defined as the peak of the T wave. The RT end interval (RTend) was defined as the time between the peak of the R wave and the maximum negative derivative of the T wave. T peak-end (T(p-e)) was defined as the time between the T peak and the maximum negative derivative of the T wave (Fig. 1). RT dispersion was automatically calculated as the difference between the longest RT interval (RTmax) and the shortest RT interval (RTmin). RTend dispersion was automatically calculated as the difference between the longest RTend interval (RTend max) and the shortest RTend interval (RTend min). T peak-end dispersion was also automatically calculated as the difference between the longest T peak-end interval (Tp-e max) and the shortest T peak-end interval (Tp-e min). The corrected RT interval (RT-c), corrected RTend interval (RTend-c), and corrected T peak-end interval (T(p-e)-c) were calculated according to the Bazett formula. Average RT-c, average RTend-c, and average T(p-e)-c were calculated as the average value of each of these variables as detected on the 187-channel SAVP-ECG. Formulas for the variables are as follows:

Average RT-c = average of each RT-c
RT-c dispersion = RT-c max − RT-c min
Average RTend-c = average of each RTend-c
RTend-c dispersion = RTend-c max − RTend-c min
Average T(p-e)-c = average of each T(p-e)-c
T(p-e)-c dispersion = T(p-e)-c max − T(p-e)-c min
Average RT-c dispersion = average of (each RT-c − RT min-c)
Average RTend-c dispersion = average of (each RTend-c − RTend min-c)
Average T(p-e)-c dispersion = average of [each T(p-e)-c − T(p-e)-c min]

The RTc, RTe-c, and T(p-e)-c maps were displayed as 256-color coordinated maps according to the time difference. In brief, blue represents < 40 ms; green-yellow, 40 − 79 ms; orange, 80 − 99 ms; and red ≥ 100 ms.

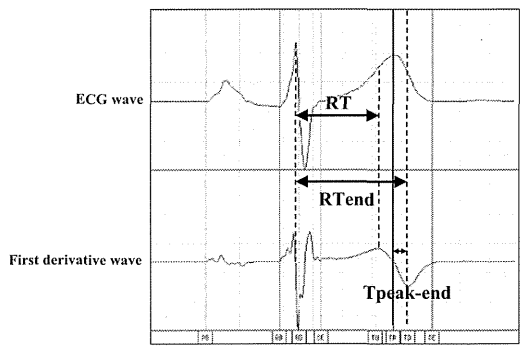

Fig. 1. Reference point for RT interval, T peak-end interval, and RTend interval. The RT interval was defined as the time between the peak point of the R wave and the positive maximum peak of the first derivative of the T wave. The T peak-end was defined as the time between the peak point of the T wave and the negative maximum peak of the first derivative of the T wave. RTend was defined as the time between the peak point of the R wave and the negative maximum peak of the first derivative of the T wave (modified from Nakai et al. [9]).

2.4. Depolarization

The modified *X–Y–Z*-lead ECG and the synthesized signals from the 187-channel SAVP-ECGs were amplified and passed through a finite impulse response (FIR) digital filter (frequency characterization: 27th order) with a low frequency of 45 Hz and a high frequency of 280 Hz, and then A/D converted with 12-bit accuracy at 2000 samples/s. After rejection of ectopic beats, ECG signals over 10 min were averaged by means of the signal-processing system. The non-filtered *X–Y–Z*-lead ECG, filtered *X–Y–Z*-lead ECG, and vector magnitude ECG were displayed on the same time scale (Fig. 1). The filtered QRS (fQRS) duration was determined automatically according to the beginning and end of the vector magnitude ECG by the points exceeding 5 times the noise levels. The root mean square of the last 40 ms (RMS_{40}) was measured by the integrated magnitude at 40 ms before the QRSend of the vector magnitude ECG. In addition, we measured the duration of low-amplitude signals < 40 μV (LAS_{40}) on the vector magnitude ECG. Spatial distribution of integrated high-frequency late potentials (HFLPs), as shown by 187-channel SAVP-ECG mapping, was calculated as the integration of the electrical potentials of fQRS measured between 30 ms (initial offset) before the QRSend (QRSend-30) and the QRSend. The endpoint in each channel was defined as the endpoint of the QRS, where the average exceeded the mean plus 5 standard deviations of the noise sample. The integrated HFLP map based on the 187-channel SAVP-ECGs was defined graphically by the gray scale that exceeded 5 times the mean noise level. The spatial distribution of integrated HFLPs based on the 187-channel SAVP-ECGs was superimposed on the RTc and T(p-e)-c dispersion map (Fig. 2).

2.5. Electrophysiological study

A comprehensive electrophysiological study was performed in 27 patients in a fasting, drug-free, non-sedated state. For patients who underwent coronary artery stent implantation, programmed ventricular stimulation was performed at 1 month after stent implantation. After obtaining access to the right femoral vein at 4 sites, 1 quadripolar catheter (Biosense-Webster, Diamond Bar, CA, USA) was positioned at the right atrial appendage, 1 octapolar catheter (Biosense-Webster) was positioned at the his bundle electrogram recording site, and 2 steerable quadripolar catheters (6 F) with an interelectrode distance of 2–5–2 mm (Biosense-Webster) were positioned in the right ventricular apex and outflow tract. Endocardial potentials were filtered to recording frequencies of 30 − 500 Hz and recorded on a BARD computer system (BARD Lab Pro, BARD Electrophysiology, Lowell, MA, USA). Programmed electrical stimulation

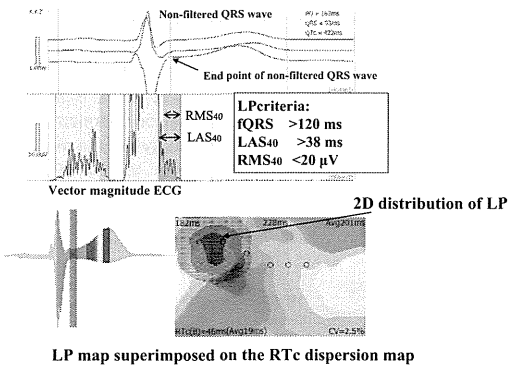

Fig. 2. Spatial distribution of high frequency ventricular late potentials (HFLPs) as defined by the gray scale on the RT dispersion map based on a 187-channel signal-averaged vector-projected high-resolution electrocardiogram. HFLPs were generated graphically by dividing voltages that exceeded 5 times the mean noise level, and represented by an increasing gray scale. The HFLP area is variable depending on the threshold voltage, which can be changed in 0.5 μV steps. Note the high frequency late potentials located at the right anterior lesion. The RTc dispersion map was displayed as a 256-color coordinated map according to the time differences. In brief, the blue represents < 40 ms; green-yellow, 40 – 79 ms; orange, 80 – 99 ms; and red, ≥ 100 ms. LP, ventricular late potential; fQRS, filtered QRS duration; RMS_{40}, root mean square of the last 40 ms; LAS_{40}, duration of low amplitude signals < 40 μV; RTc, time between the peak point of the R wave and the positive maximum peak of the first derivative of the T wave corrected using the Bazett formula.

from the right ventricular apex and right ventricular outflow tract was performed at twice the diastolic threshold strength and a pulse of 2-ms duration with a pulse generator (BD-02, Fukuda Denshi Co.). An S_1–S_2 interval was applied after 8 beats of drive pacing (S_1) at basic cycle lengths of 600 ms and 400 ms. The S_1–S_2 interval was decreased in 10-ms steps until the effective refractory period of the right ventricle was reached. When ventricular fibrillation (VF) lasting > 5 s and requiring DC shock was not induced with a single premature beat, 3 extra stimuli (S_2 until the effective refractory period was reached, S_3 and S_4 to 180 ms) were delivered.

2.6. Follow-up

In general, patients were followed up at 4- to 5-month intervals in our outpatient clinic. Examinations included assessment of subjective symptoms and 12-lead ECG and device interrogation if necessary in the event of onset of symptoms or device discharges. Follow-up ranged from 36 to 214 months (mean, 80.8 ± 52.3 months; median, 91 months).

2.7. Statistical analysis

Continuous clinical and electrophysiological values are shown as mean ± SD. Between-group differences in these values were analyzed using the Mann–Whitney *U* test. Categorical data were analyzed by Fisher's exact probability test. A *P* value of < 0.05 was considered statistically significant. StatView 5.0 software (SAS Institute Inc., Cary, NC, USA) was used for analysis.

3. Results

The clinical, genetic, electrocardiographic, and electrophysiological characteristics of the study patients are shown in Table 1. Eight of the 45 patients were symptomatic, having a history of syncope (n=3) or aborted SCD (n=5). The remaining 37 patients were asymptomatic, although 4 had a family history of SCD. The ECGs of 26 patients showed a type 1 basal ECG pattern, and 19 showed a type 1 ECG pattern after a challenge test. An SCN 5 A mutation was found in 1 patient. Positive ventricular late potentials were detected in 26 of 44 (59.1%) patients. Among the 28 patients in whom an electrophysiological study was performed, VF was induced in 25 (89.3%). The clinical, genetic, electrocardiographic, and electrophysiological characteristics of the patients in each group (symptomatic and asymptomatic patients) are shown in Table 2. A family history of sudden cardiac death (SCD) at age < 45 years, spontaneous type 1 ECG, and positive ventricular late potentials were significantly more prevalent in the group of symptomatic patients. However, the AH interval, HV interval, and inducibility of VF/polymorphic VT did not differ between the 2 groups of patients.

Table 1
Clinical, genetic, electrocardiographic, and electrophysiological characteristics of the study patients (n=45).

Age (y); mean ± SD	51.5 ± 14.3
Sex ratio (M/F)	43/2
Symptomatic	8
Cardiopulmonary arrest	5
Syncope	3
Family history of SCD	4
Spontaneous Brugada type 1 ECG pattern	26
SCN5A gene mutation	1
Late potential; mean ± SD	26/44 (59.1%)
EPS	28
AH interval (ms); mean ± SD	101.5 ± 22.7
HV interval (ms); mean ± SD	47.4 ± 9.2
Inducible VF/PVT at EPS	25
ICD implantation	10
Follow-up (mo); mean ± SD	80.8 ± 52.3
Arrhythmic event during follow-up	1

Number of patients is shown unless otherwise indicated.
SCD, sudden cardiac death; EPS, electrophysiological study; VF, ventricular fibrillation; PVT, polymorphic ventricular tachycardia; ICD, implantable cardioverter defibrillator.

3.1. Spatial and transmural repolarization obtained from 187-channel SAVP-ECG

The average RT-c, RTend-c, and T(p-e)-c intervals calculated from the 187-channel SAVP-ECG are shown in Table 3. The average T(p-e)-c was marginally increased in patients with a type 1 ECG compared to that in patients with a type 2/3 ECG (49.0 ± 14.1 ms vs. 41.0 ± 8.1 ms, P=0.062). However, no significant difference between average RTend-c and average T(p-e)-c intervals was observed.

3.2. Spatial and transmural dispersion of repolarization obtained from 187-channel SAVP-ECG

RT-c dispersion was significantly greater in patients with a type 1 ECG compared to that in patients with a type 2/3 ECG (86.3 ± 20.8 ms vs. 73.3 ± 19.7 ms, P=0.041). Additionally, average RT-c dispersion was greater in patients with a type 1 ECG compared to that in patients with a type 2/3 ECG (41.8 ± 15.8 ms vs. 32.4 ± 16.8 ms, P=0.064) (Table 4, Figs. 3 and 4). However, no significant difference in RTe-c dispersion, average RTe-c dispersion, T(p-e)-c dispersion, or average T(p-e) dispersion was observed between the type 1 and type 2/3 ECG patterns. No significant difference in RT-c dispersion, average RT-c dispersion, RTe-c dispersion, average RTe-c dispersion, T(p-e) dispersion, or average T(p-e) dispersion was observed between symptomatic and asymptomatic patients (Table 4).

An arrhythmic event occurred in 1 symptomatic patient during the follow-up period.

4. Discussion

In the present study, we showed that average T(p-e)-c interval, RT-c dispersion, and corrected average repolarization dispersion were greater in patients with a type 1 ECG than in patients with a type 2/3 ECG. However, no differences were noted in other variables representing other parameters of repolarization interval and spatial and transmural dispersion of repolarization between patients with a type 1 and those with a type 2/3 ECG. Furthermore, no differences in spatial and transmural dispersion variables were observed between symptomatic and asymptomatic patients, although the prevalence of positive late ventricular potentials was significantly higher in symptomatic patients. The prevalence of positive ventricular late potential in type 1 ECG was marginally higher compared to that in type 2/3 ECG (16/26 vs. 6/18, $P=0.062$), and both repolarization and depolarization abnormalities may constitute a type 1 ECG. Qualitative analysis showed that late potentials were located adjacent to the V_2–V_3 ECG position, whereas the distribution of the RT-c, RTe-c, and T(p-e)-c

Table 2
Clinical, genetic, electrocardiographic, and electrophysiological characteristics of symptomatic and asymptomatic patients.

	Symptomatic ($n=8$)	Asymptomatic ($n=37$)	*P* value
Age (y); mean ± SD	56.0 ± 16.0	49.2 ± 13.1	0.18
Sex ratio (M/F)	8/0	35/2	0.50
Family history of SCD	3	1	0.014
Spontaneous Brugada type 1 ECG pattern	8	18	0.0072
Late potential	7/8	16/36	0.023
SCN5A gene mutation	1	0	0.178
EPS	8	19	0.014
AH interval (ms); mean ± SD	92.9 ± 9.2	105.1 ± 25.8	0.36
HV interval (ms); mean ± SD	48.5 ± 3.8	47.7 ± 11.1	0.66
Inducible VF/PVT at EPS	8/8	17/19	0.34
ICD implantation	5	5	0.0025
Follow-up (mo); mean ± SD	124 ± 65	71.5 ± 45.0	0.0005
Arrhythmic event during follow-up	1	0	Not applicable

Number of patients is shown unless otherwise indicated.
SCD, sudden cardiac death; EPS, electrophysiological study; VF, ventricular fibrillation; PVT, polymorphic ventricular tachycardia; ICD, implantable cardioverter defibrillator.

Table 3
Comparison of spatial and transmural repolarization time and Brugada ECG type and symptoms.

	Avg. RT-c	Avg. RTe-c	Avg. T(p-e)-c
BS Type 1 ECG	215.7 ± 24.5	312.9 ± 24.0	49.0 ± 14.1
BS Type 2/3 ECG	215.1 ± 27.9	301.4 ± 33.2	41.0 ± 8.1
***P* value**	0.93	0.11	0.062
Symptomatic	213.9 ± 40.3	310.4 ± 35.3	48.5 ± 11.1
Asymptomatic	215.8 ± 21.0	307.5 ± 52.8	45.2 ± 12.9
***P* value**	0.47	0.73	0.41

RT-c, corrected recovery time interval; Avg., average; RTe-c, corrected recovery time end interval; T(p-e), T peak-end interval.
See the text for the definition of these parameters.

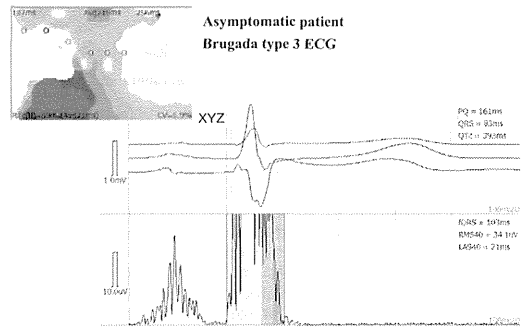

Fig. 3. RTc dispersion map in an asymptomatic patient with a Brugada type 3 ECG. Color scale is as described in Fig. 2. RTc dispersion is 69 ms, and average RTc dispersion is 23 ms. The ventricular late potential is negative. Abbreviations are as in Fig. 2.

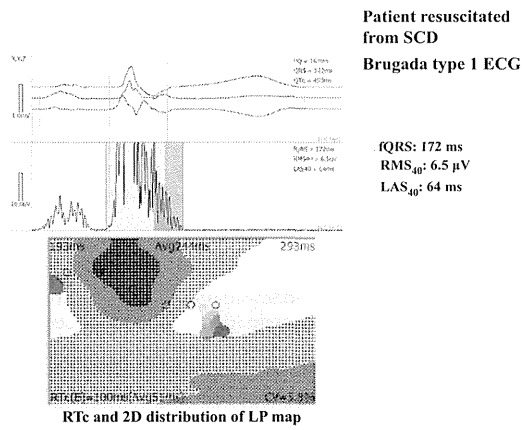

Fig. 4. RTc dispersion map in a symptomatic case with a Brugada type 1 ECG. Color scale is as in Fig. 2. RTc dispersion is 100 ms and average RTc dispersion is 51 ms. The ventricular late potential is positive. Abbreviations are as in Fig. 2.

Table 4
Comparison of spatial and transmural dispersion of repolarization and Brugada ECG type and symptoms.

	RT-c dispersion	Avg. RT-c dispersion	RTe-c dispersion	Avg. RTe-c dispersion	T(p-e)-c dispersion	Avg. T(p-e)-c dispersion
BS Type 1 ECG	86.3 ± 20.8	41.8 ± 15.8	64.2 ± 18.0	37.6 ± 17.8	62.4 ± 19.3	37.6 ± 18.7
BS Type 2/3 ECG	73.3 ± 19.7	32.4 ± 16.8	73.3 ± 19.7	33.8 ± 10.9	58.8 ± 13.3	35.8 ± 11.8
***P* value**	0.041	0.064	0.17	0.42	0.49	0.72
Symptomatic	77.6 ± 28.4	41.3 ± 17.4	67.8 ± 13.1	30.9 ± 12.7	59.6 ± 19.7	27.6 ± 13.7
Asymptomatic	81.9 ± 19.6	37.4 ± 16.7	60.1 ± 16.9	37.2 ± 15.8	61.3 ± 16.7	38.8 ± 16.1
***P* value**	0.61	0.56	0.24	0.30	0.80	0.74

RT-c, corrected recovery time interval; Avg., average; RTe-c, corrected recovery time end interval; T(p-e), T peak-end interval.
See the text for the definition of these parameters.

dispersion was more widespread, and usually located left inferior to the late potential location. The dispersion of the depolarization and repolarization indices suggests a different pathogenesis of these abnormalities.

Transmural dispersion of repolarization within the ventricular myocardium has been suggested to underlie arrhythmogenesis in Brugada, short QT, or long QT syndrome, and in SCD [12,13]. Three electrophysiologically distinct cell types have been identified in the ventricular myocardium: endocardial, epicardial, and M cells. Differences in the time course of repolarization of these 3 ventricular myocardial cell types contribute prominently to inscription of the electrocardiographic T-wave [14]. In isolated ventricular wedge preparations, the peak of the T-wave was shown to coincide with epicardial repolarization and the end of the T-wave with repolarization of the M cells; thus, Tp-e provides a measure of transmural dispersion of repolarization [15]. These and other studies have suggested that although Tp-e on the surface ECG may not be equivalent to transmural dispersion of repolarization, this interval may serve as an index of transmural dispersion of repolarization and thus be helpful in forecasting risk for the development of life-threatening arrhythmias [13,15]. Evidence in support of this hypothesis has been provided in hypertrophic cardiomyopathy, congenital, and acquired long QT syndrome, and other pathologic conditions [7]. The reported cellular basis of BS is marked dispersion of repolarization in the right ventricular epicardium and transmurally [16–18]. Previous studies showed that the T peak-end interval and T peak-end dispersion on the 12-lead ECG are potential risk factors for VT/VF and VT/VF inducibility in patients with the Brugada ECG phenotype [8,19]. Studies have reported that QT/RR and T peak-end/RR slopes show loss of rate-dependency in VF(+) BS patients than in VF(−) BS patients and control patients, and the T peak-end interval correlated negatively with the RR interval in the VF(+) Brugada group and positively with the RR interval in the VF(−) Brugada and control groups [20]. However, an experimental study comparing epicardial electrograms and surface electrograms showed that T peak-end does not correlate with transmural dispersion of repolarization but rather is an index of total dispersion of repolarization [21]. In the present study, average T(p-e)-c interval, corrected maximum T peak-end dispersion, and corrected average T peak-end dispersion from the 187-channel SAVP-ECG did not differ between symptomatic and asymptomatic BS patients. However, average T(p-e)-c interval was marginally increased in patients with type 1 ECG compared to that in patients with type 2/3 Brugada type ECG. Additionally, corrected maximum RT interval dispersion and corrected average RT interval dispersion were greater in patients with a type 1 ECG compared to those in patients with a type 2/3 Brugada type ECG. However, the parameters on the absolute value and dispersion of repolarization did not differ between symptomatic and asymptomatic BS patients. Therefore, the ECG manifestation of type 1 Brugada ECG may be related to the longer transmural repolarization interval and greater spatial dispersion of refractoriness. Recent studies have shown that right ventricular fibrosis and conduction delay without a transmural repolarization gradient are the dominant pathophysiologic mechanisms for type 1 ECG and the origin of VF in BS [22–25]. We previously reported the presence of right ventricular outflow tract endocardial conduction delay and right ventricular septal histopathological abnormalities in patients with BS [26,27]. Furthermore, Nademanee et al. reported that the electrophysiological mechanism in patients with BS is delayed depolarization over the anterior aspect of the right ventricular outflow tract, and catheter ablation of this area of abnormal depolarization results in normalization of the Brugada ECG pattern and prevents VT/VF [28]. In our patient series, the prevalence of ventricular late potentials was significantly higher in symptomatic patients than in asymptomatic patients.

4.1. Study limitations

Our study was limited first by the fact that the 187-channel SAVP-ECG is not yet widely accepted for assessment of spatial and transmural dispersion of repolarization; therefore, further studies may be needed to validate this novel ECG algorithm. Second, the study group was small. A subsequent study involving a large study group is needed to verify the clinical usefulness of the 187-channel SAVP-ECG.

5. Conclusion

Spatial dispersion of repolarization may constitute the electrocardiographic pattern of the Brugada type ECG, and this conduction disturbance in addition to repolarization abnormality may contribute to the development of malignant ventricular tachyarrhythmias.

Conflict of interest

None.

References

[1] Brugada P, Brugada J. Right bundle branch block, persistent ST segment elevation and sudden cardiac death: a distinct clinical and electrocardiographic syndrome. A multicenter report. J Am Coll Cardiol 1992;20:1391–6.
[2] Benito B, Brugada R, Brugada J, et al. Brugada syndrome. Prog Cardiovasc Dis 2008;51:1–22.
[3] Antzelevitch C, Brugada P, Borggrefe M, et al. Brugada syndrome: report of the second consensus conference: endorsed by the Heart Rhythm Society and the European Heart Rhythm Association. Circulation 2005;111:659–70.
[4] Priori SG, Napolitano C, Gasparini M, et al. Clinical and genetic heterogeneity of right bundle branch block and ST-segment elevation syndrome: a prospective evaluation of 52 families. Circulation 2000;102:2509–15.
[5] Eckardt L, Probst V, Smits JP, et al. Long-term prognosis of individuals with right precordial ST-segment-elevation Brugada syndrome. Circulation 2005;111:257–63.
[6] Brugada J, Brugada R, Brugada P. Determinants of sudden cardiac death in individuals with the electrocardiographic pattern of Brugada syndrome and no previous cardiac arrest. Circulation 2003;108:3092–6.
[7] Antzelevitch C. Role of spatial dispersion of repolarization in inherited and acquired sudden cardiac death syndrome. Am J Physiol Heart Circ Physiol 2007;293:H2024–38.
[8] Castro Hevia J, Antzelevitch C, Tornés Barzaga F, et al. Tpeak-Tend and Tpeak-Tend dispersion as risk factors for ventricular tachycardia/ventricular fibrillation in patients with the Brugada syndrome. J Am Coll Cardiol 2006;47:1828–34.
[9] Nakai K, Tsuboi J, Okabayashi H, et al. Development of a signal-averaged vector-projected 187-channel high-resolution electrocardiogram for the evaluation of the spatial location of high-frequency potentials and abnormal ventricular repolarization. Int Heart J 2007;48:701–13.
[10] Nakai K, Miyake F, Kasanuki H, et al. Newly developed signal-averaged vector-projected 187-channel electrocardiogram can evaluate the spatial distribution of repolarization heterogeneity. Int Heart J 2008;49:153–64.
[11] Suzuki A, Shiga T, Nakai K, et al. Interlead difference between T-peak to T-end intervals in resynchronization patients with an implantable cardioverter-defibrillator. J Electrocardiol 2010;43:706–12.
[12] Antzelevitch C. Tpeak-Tend interval as an index of transmural dispersion of repolarization. Eur J Clin Invest 2001;31:555–7.
[13] Panikkath R, Reinier K, Uy-Evanado A, et al. Prolonged Tpeak-to-Tend interval on the resting ECG is associated with increased risk of sudden cardiac death. Circ Arrhythm Electrophysiol 2011;4:441–7.
[14] Yan GX, Antzelevitch C. Cellular basis for the normal T wave and the electrocardiographic manifestation of the long QT syndrome. Circulation 1998;98:1928–36.
[15] Fish JM, Di Diego JM, Nesterenko V, et al. Epicardial activation of left ventricular wall prolongs QT interval and transmural dispersion of repolarization: implications for biventricular pacing. Circulation 2004;109:2136–42.
[16] Yan GX, Antzelevitch C. Cellular basis for the Brugada syndrome and other mechanisms of arrhythmogenesis associated with ST-segment elevation. Circulation 1999;100:1660–6.
[17] Aiba T, Shimizu W, Hidaka I, et al. Cellular basis for trigger and maintenance of ventricular fibrillation in the Brugada syndrome model. J Am Coll Cardiol 2006;47:2074–85.
[18] Morita H, Zipes DP, Fukushima-Kusamo K, et al. Repolarization heterogeneity in the right ventricular outflow tract: correlation with ventricular arrhythmias in Brugada patients and in an in vitro Brugada model. Heart Rhythm 2008;5:725–33.

[19] Letsas KP, Weber R, Asthemer K, et al. Tpeak-Tend interval and Tpeak-Tend/QT ratio as markers of ventricular tachycardia inducibility in subjects with Brugada ECG phenotype. Europace 2010;12:271–4.
[20] Sangawa M, Morita H, Nakatsu T, et al. Abnormal transmural repolarization process in patients with Brugada syndrome. Heart Rhythm 2009;6:1163–9.
[21] Opthof T, Coronel R, Wilms-Schopman FJ, et al. Dispersion of repolarization in canine ventricle and the electrocardiographic T wave: Tp-e interval does not reflect transmural dispersion. Heart Rhythm 2007;4:341–8.
[22] Coronel R, Casini S, Koopmann TT, et al. Right ventricular fibrosis and conduction delay in a patient with clinical signs of Brugada syndrome. A combined electrophysiological, genetic, histopathologic, and computational study. Circulation 2005;112:2769–77.
[23] Postema PG, van Dessel PF, de Bakker JM, et al. Slow and discontinuous conduction conspire in Brugada syndrome: a right ventricular mapping and simulation study. Circ Arrhythm. Electrophysiol 2008;1:379–86.
[24] Postema PG, van Dessel PF, Kors JA, et al. Local depolarization abnormalities are the dominant pathophysiologic mechanism for type 1 electrocardiogram in Brugada syndrome: a study of electrocardiograms, vectorcardiograms, and body surface potential maps during ajmaline provocation. J Am Coll Cardiol 2010;55:789–97.
[25] Hoogendijk MG, Potse M, Linnenbank AC, et al. Mechanism of right precordial ST-segment elevation in structural heart disease: excitation failure by current-to-load mismatch. Heart Rhythm 2010;7:238–48.
[26] Ohkubo K, Watanabe I, Takagi Y, et al. Endocardial electrograms from the right ventricular outflow tract after induced ventricular fibrillation in patients with Brugada syndrome. Circ J 2007;71:1258–62.
[27] Ohkubo K, Watanabe I, Okumura Y, et al. Right ventricular histological substrate and conduction delay in patients with Brugada syndrome. Int Heart J 2010;51:17–23.
[28] Nademanee K, Veerakul G, Chadanamattha P, et al. Prevention of ventricular fibrillation episodes in Brugada syndrome by catheter ablation over the anterior right ventricular outflow tract epicardium. Circulation 2011;123:1270–9.

Sudden cardiac arrest recorded during Holter monitoring: Prevalence, antecedent electrical events, and outcomes

Eiichi Watanabe, MD,[*] Teruhisa Tanabe, MD, PhD,[†] Motohisa Osaka, MD,[‡] Akiko Chishaki, MD,[§] Bonpei Takase, MD, FACC, FAHA,[‖] Shinichi Niwano, MD,[#] Ichiro Watanabe, MD,[**] Kaoru Sugi, MD,[††] Takao Katoh, MD,[‡‡] Kan Takayanagi, MD, FACC, FHRS,[§§] Koushi Mawatari, MD,[‖‖] Minoru Horie, MD,[##] Ken Okumura, MD,[***] Hiroshi Inoue, MD,[†††] Hirotsugu Atarashi, MD, FESC,[‡‡‡] Iwao Yamaguchi, MD, FACC,[§§§] Susumu Nagasawa, MD,[‖‖‖] Kazuo Moroe, MD,[###] Itsuo Kodama, MD,[****] Tsuneaki Sugimoto, MD,[††††] Yoshifusa Aizawa, MD[‡‡‡‡]

From the [*]Department of Cardiology, Fujita Health University School of Medicine, Toyoake, Japan, [†]Department of Cardiology, Tokai University School of Medicine, Isehara, Japan, [‡]Department of Basic Science, Nippon Veterinary and Life Science University, Tokyo, Japan, [§]Department of Health Sciences, Faculty of Medical Sciences, Kyushu University, Fukuoka, Japan, [‖]Department of Intensive Care Unit, National Defense Medical College, Tokorozawa, Japan, [#]Department of Cardiovascular Medicine, Kitasato University School of Medicine, Sagamihara, Japan, [**]Division of Cardiology, Department of Medicine, Nihon University School of Medicine, Tokyo, Japan, [††]Division of Cardiovascular Medicine, Toho University Ohashi Medical Center, Tokyo, Japan, [‡‡]International University of Health and Welfare, Mita Hospital, Tokyo, Japan, [§§]Department of Cardiology, Dokkyo Medical University Koshigaya Hospital, Koshigaya, Japan, [‖‖]Department of Cardiology, Kagoshima Seikyo Hospital, Kagoshima, Japan, [##]Department of Cardiovascular and Respiratory Medicine, Shiga University of Medical Science, Otsu, Japan, [***]Department of Cardiology, Hirosaki University Graduate School of Medicine, Hirosaki, Japan, [†††]Second Department of Internal Medicine, Toyama University Hospital, Toyama, Japan, [‡‡‡]Department of Cardiology, Nippon Medical School, Tama-Nagayama Hospital, Tokyo, Japan, [§§§]Tsukuba University School of Medicine, Tsukuba, Japan, [‖‖‖]Cardiovascular Division, Department of Internal Medicine, Hyogo College of Medicine, Nishinomiya, Japan, [###]Fukuoka University School of Medicine, Fukuoka, Japan, [****]Nagoya University, Nagoya, Japan, [††††]Kanto Central Hospital, Tokyo, Japan, and [‡‡‡‡]Division of Research and Development, Tachikawa Medical Center, Nagaoka, Japan.

BACKGROUND Causative arrhythmias of sudden cardiac arrest (SCA) are changing in this age of improved coronary care.

OBJECTIVE The purpose of this study was to examine the frequency of terminal arrhythmias and the electrical events prior to SCA.

METHODS We analyzed 24-hour Holter recordings of 132 patients enrolled from 41 institutions who either died (n = 88) or had an aborted death (n = 44). The Holter recordings were obtained for diagnosing and evaluating diseases and arrhythmias in those without any episodes suggestive of SCA.

RESULTS In 97 patients (73%), SCA was associated with ventricular tachyarrhythmias and in 35 (27%) with bradyarrhythmias. The bradyarrhythmia-related SCA patients were older than those with a tachyarrhythmia-related SCA (70 ± 13 years vs 58 ± 19 years, $P < .001$). The most common arrhythmia for a tachyarrhythmia-related SCA was ventricular tachycardia degenerating to ventricular fibrillation (45%). The bradyarrhythmia-related SCA was caused by asystole (74%) or AV block (26%). Spontaneous conversion was observed in 37 patients (38%) with ventricular tachyarrhythmias. Of those, 62% of the patients experienced symptoms including syncope, chest pain, or convulsion. Multivariate logistic analysis revealed that independent predictors of mortality for tachyarrhythmia-related SCAs were advanced age (odds ratio 1.04, 95% confidence interval 1.02–1.08) and ST elevation within the hour before SCA (odds ratio 3.54, 95% confidence interval 1.07–13.5). In contrast, the presence of

This work was supported by the Vehicle Racing Commemorative Foundation and Suzuken Memorial Foundation. This work does not have any relationships with the industries. Dr. Watanabe received speaker fees from Bayer and Boehringer Ingelheim. Dr. Katoh received consultant fees from Kissei Pharmaceutical and Dai Nippon Sumitomo Pharmaceutical; and received manuscript fee from Astellas and Ono Pharmaceutical. Dr. Sugi received scholarship funds from Sanofi Aventis, Mochida Pharmaceutical, Daiichi Sankyo, and Dai Nippon Sumitomo Pharmaceutical; and speaker fees from Bayer and Boehringer Ingelheim. Dr. Atarashi received consultant fees from Teijin and Otsuka Pharmaceutical and Eisai; received speaker fees from Daiichi Sankyo, Boehringer Ingelheim, and Bayer; and received research funds from Boehringer Ingelheim. **Address reprint requests and correspondence:** Dr. Eiichi Watanabe, Department of Cardiology, Fujita Health University School of Medicine, 1-98 Dengakugakubo, Kutsukake-cho, Toyoake, Aichi 470-1192, Japan. E-mail address: enwatan@fujita-hu.ac.jp.

 http://dx.doi.org/10.1016/j.hrthm.2014.04.036

preceding torsades de pointes was associated with spontaneous conversion (odds ratio 0.20, 95% confidence interval 0.05–0.66).

CONCLUSION The most frequent cause of SCA remains ventricular tachyarrhythmias. Advanced age and ST elevation before SCA are risk factors for mortality in tachyarrhythmia-related SCAs.

KEYWORDS Electrocardiogram; Sudden death; Arrhythmia; Survivor; Holter recording

ABBREVIATIONS **AAD** = antiarrhythmic drug; **AV** = atrioventricular; **CI** = confidence interval; **ECG** = electrocardiogram; **OR** = odds ratio; **PVC** = premature ventricular complex; **SCA** = sudden cardiac arrest; **TdP** = torsades de pointes; **VF** = ventricular fibrillation; **VT** = ventricular tachycardia; **VTA** = ventricular tachyarrhythmia

(Heart Rhythm 2014;11:1418–1425)

Introduction

Sudden cardiac arrest (SCA) is one of the major causes of death in industrialized countries and is an important clinical and public health problem.[1,2] SCAs annually cause approximately 300,000 deaths in the United States[3–5] and 70,000 in Japan[6,7] in out-of-hospital settings. An early systematic review of Holter monitoring showed that SCAs result mainly from ventricular tachyarrhythmias (VTAs), which include ventricular tachycardia (VT) and ventricular fibrillation (VF), and in part from primary bradyarrhythmias.[8] Recent studies using data from emergency rescue services reported a reduction in the prevalence of SCAs due to VTAs and hypothesized that this was a consequence of a decline in coronary artery disease mortality in the last 2 decades.[9–11] However, most existing analyses have been limited to patients who received an attempted resuscitation.[7,9,10,12] Additionally, it is difficult to accurately identify the arrhythmia responsible for a given SCA based on the initial rhythm recorded by emergency personnel. The reason for this is an arrhythmia can start via one mechanism and morph into another. Studies using data from implantable cardioverter-defibrillators also are suboptimal because a high-fidelity electrogram during the hours that precede the onset of the SCA cannot be stored because of a limited memory storage capacity. In contrast, a Holter electrocardiogram (ECG) recording is a comprehensive tool that can provide definitive information about antecedent electrical events and terminal arrhythmias leading to SCA.[8,13–19]

The aim of the present study were 3-fold: (1) to reexamine the prevalence of terminal arrhythmias in this age of improved treatment of, and a diminished morbidity from, coronary artery disease; (2) to identify the ECG markers that precede the onset of SCA by scrutinizing the last hour before SCA in the Holter recordings and to identify the independent predictors of aborted death for VTAs; and (3) to examine the characteristics of spontaneous termination of VTAs.

Methods

Patients

We examined the Holter recordings of 132 patients enrolled from 41 institutions in Japan from 1990 to 2013. This study included 85 patients previously published in the proceedings of sudden cardiac death workshops held in 1991[20] and 2010.[21] The remaining 47 patients were enrolled after those workshops. Thirty-two patients were reported in both the 2010 workshop and two heart rate variability–related articles.[22,23]

Patients were enrolled if they required Holter monitoring for any reason, whether they were outpatients or patients hospitalized for diagnostic testing. Patients who received Holter monitoring during their stay in coronary care units or during hospitalization for end-state disease were excluded. The protocol was approved by the ethics committee of each institution, and patients or their families gave written informed consent at the time of Holter recording. The study complied with the Declaration of Helsinki.

Holter recording analysis

Holter recording was done using the bipolar CM5 chest lead and a modified lead II. A full ECG printout and rhythm strip at a paper speed of 25 mm/s was collected to the extent possible. Three authors (EW, TT, YA) reevaluated each case to identify the terminal arrhythmia and outcome by reviewing the Holter recordings with differences resolved by consensus. A pediatric cardiologist made a diagnosis of the pediatric Holter recording. The arrhythmias considered during the hour before SCA (preceding electrical events) included tachycardia with any rhythm having a rate ≥ 100 bpm, bradycardia with any rhythm having a rate ≤ 50 bpm, sinus pauses with a duration ≥ 3 seconds, atrioventricular (AV) block, paroxysmal atrial fibrillation, and a high frequency (≥ 10 per hour) of premature atrial complexes or premature ventricular complexes (PVCs). Paroxysmal atrial fibrillation was defined as an arrhythmia of a supraventricular origin associated with a grossly irregular ventricular rhythm and no visible P waves that lasted for ≥ 10 seconds. VT was considered present when at least 3 consecutive PVCs occurred at a rate ≥ 120 bpm. VF required a disorganized ventricular rhythm with no discrete QRS complexes. Torsades de pointes (TdP) was defined as a distinctive form of polymorphic VT characterized by smooth changes in the amplitude and twisting of the QRS complexes around the isoelectric line. The R-on-T phenomenon was defined as a superimposition of a PVC on the T wave of a preceding beat. T-wave alternans was defined as alternans in either the amplitude or the shape of the T wave. Any ST elevation ≥ 1 mm or ST depression ≤ -1 mm for ≥ 10 seconds was considered to be a reflection of ischemia. Finally, we noted whether the cardiac rhythm was reestablished, and whether or not the patient survived. Several preceding electrical events were observed in each patient, but they had only 1 terminal arrhythmia before SCA. The tachycardic terminal arrhythmia types were categorized into 4 types, namely, as

VT degenerating to VF (VT/VF type), VF without any antecedent VT (primary VF type), TdP, or VT throughout the arrest (VT type). The bradycardic terminal arrhythmia types were classified into asystole or AV block.

Definition

We employed a commonly used definition of SCA, that is, death from an unexpected circulatory arrest, due to a cardiac arrhythmia occurring within an hour of the onset of symptoms.[1] The survivors in this study had aborted death that was defined as either VTAs lasting ≥ 1 minute or pauses lasting ≥ 10 seconds but terminating spontaneously or being reversed by resuscitation and leading to the patient's survival. For the purpose of analyzing the circadian distribution of SCA, the SCA event time was defined as the time of day when the final, lethal arrhythmia began, whether or not it was aborted.

Statistical analysis

Differences in the frequency were tested using the χ^2 test or the Fisher exact t test for categorical data. A Student t test or 1-way analysis of variance was used to evaluate continuous variables, where appropriate. Arrhythmias were analyzed as dichotomous outcomes. Stepwise multiple logistic regression analyses were performed to determine which potential variables had significant effects on each of the outcome variables by controlling for other significant variables. Only significant variables ($P < .10$) identified in the univariate analysis were included in the starting model for the multivariate analyses. A backward elimination procedure was used to identify the final reduced model. All identified variables were included in the model, and nonsignificant covariates were removed using a backward elimination procedure according to a selection stay criterion of $P \leq .05$. An odds ratio (OR) for risk factors was assessed for a 1-unit deviation increase for the continuous variables and the condition present (vs absent) for dichotomous variables. The circadian variability of SCA was analyzed using an algorithm for a fast Fourier transform to test for the presence of periodic components. Quantitative data are expressed as mean ± SD. A 2-tailed $P < .05$ was considered significant. Statistical analysis was performed using JMP 10.0.2 software (SAS Institute, Cary, NC).

Results

Holter recordings were performed on an outpatient basis in 68% of the patients and under a hospitalized condition in 32% of the patients. The indications for Holter recordings were as follows: palpitations (51%), chest pain (29%), syncope or faintness (12%), other (15%), and unknown reasons (7%). The total exceeded 100% because of multiple indications reported.

Patient characteristics

The baseline clinical data classified according to their terminal arrhythmias are summarized in Table 1. The mean age of all patients was 61 ± 18 years (range 2–100 years). The patients with bradyarrhythmias were older and were more likely to have a history of a stroke than the VTA patients. There was no significant difference in the frequency of ischemic heart diseases between the 2 groups. All 8 of the long QT patients had VTAs as their terminal arrhythmia, but the difference in the proportion of long QT patients within

Table 1 Baseline characteristics of the patients

	Ventricular tachyarrhythmia (n = 97)	Bradyarrhythmia (n = 35)	*P* value
Age (years)	58 ± 19	70 ± 13	<.001
Male [n (%)]	61 (63)	20 (57)	.550
Basic rhythm [n (%)]			
Sinus rhythm	90 (93)	31 (89)	.440
AF	5 (5)	2 (6)	.727
Complete AV block	2 (2)	2 (6)	.286
Underlying disease [n (%)]			
Acute coronary syndrome	5 (5)	2 (6)	.727
Old myocardial infarction	18 (19)	4 (12)	.245
Effort angina	23 (24)	8 (24)	.919
Vasospastic angina	2 (2)	2 (6)	.286
Hypertension	6 (6)	6 (18)	.061
Dilated cardiomyopathy	9 (9)	1 (3)	.200
Long QT syndrome	8 (8)	0 (0)	.078
Brugada syndrome	2 (2)	0 (0)	.538
Valvular heart disease	1 (2)	3 (9)	.056
Heart failure	8 (8)	1 (3)	.256
Stroke	5 (5)	7 (20)	.015
Therapy [n (%)]			
Beta-blocker	10 (10)	3 (9)	.531
Class I AAD	16 (16)	6 (17)	.929
Class III AAD	3 (3)	0 (0)	.394
ICD implantation	1 (1)	0 (0)	.735

Data are given as mean ± SD or number (frequency).
AAD = antiarrhythmic drug; AF = atrial fibrillation; AV = atrioventricular; ICD = implantable cardioverter-defibrillator.

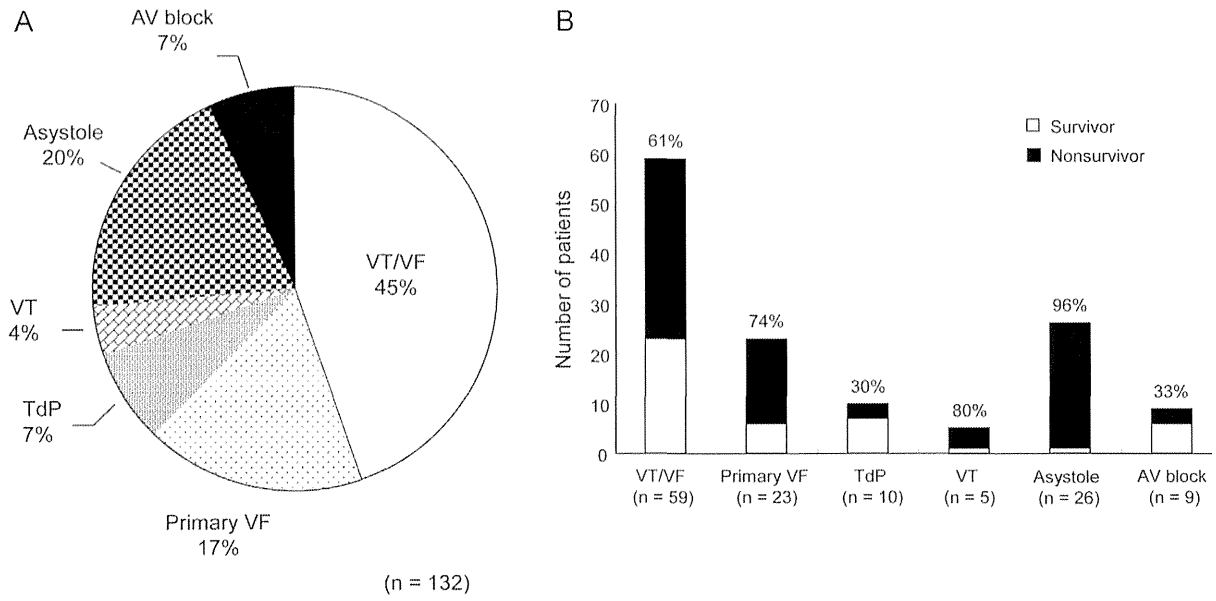

Figure 1 Frequency and outcome of terminal arrhythmias. **A:** Distribution of the types of terminal arrhythmias leading to sudden cardiac arrest or aborted death. Ventricular tachycardia degenerating into ventricular fibrillation (VT/VF) comprised most of the terminal events. Prevalence and mortality rate in relation to the terminal arrhythmias. **B:** Percentage above each arrhythmia is the mortality rate. Of the terminal tachyarrhythmias, VT/VF was found in 36 and 23, primary VF in 17 and 6, torsades de pointes (TdP) in 3 and 7, and VT in 4 and 1 for VT of the nonsurvivors and the survivors, respectively. For the terminal bradyarrhythmias, an escape rhythm was observed in 25 and 1 and AV block in 3 and 6 of the nonsurvivors and the survivors, respectively. AV = atrioventricular.

the VTA and bradyarrhythmia patients did not reach statistical significance ($P = .078$). Four patients with vasospastic angina had not received calcium channel blockers at the time of Holter recordings. The distribution of terminal arrhythmias leading to SCA is shown in Figure 1A. The VT/VF type (n = 59, 45% of all terminal arrhythmias) comprised a large portion of the terminal events followed by the primary VF type (n = 23 [17%], TdP (n = 10 [7%]), and VT type (n = 5 [4%]). The prevalence of primary bradyarrhythmic events was 27%, the sum of asystole (n = 26 [20%]) and AV block (n = 9 [7%]).

VTA patients

Baseline clinical data and preceding electrical events for the VTA patients classified according to the 4 terminal arrhythmia types are summarized in Table 2. The age and basic rhythms were similar among the 4 groups of patients. There were significant differences in the prevalence of acute coronary syndrome, hypertension, and long QT syndrome. Of the preceding electrical events, PVCs, nonsustained VT, TdP, R-on-T phenomenon, ST elevation, and ST depression were commonly observed. Significant differences were observed in the incidence of preceding electrical events including TdP and the R-on-T phenomenon.

Table 3 outlines the baseline characteristics and preceding electrical events in the VTA patients classified according to outcome. Figure 1B presents the mortality rates in relation to the terminal arrhythmias. There was no significant difference in mortality rate between the 4 VTAs ($P = .092$). Nonsurvivors were older than survivors and had a higher prevalence of heart failure than did survivors. Tachycardias and ST elevation were more frequent in nonsurvivors compared to survivors. In contrast, long QT syndrome and preceding TdP were more frequent in survivors compared to nonsurvivors. Preceding TdP was observed in 20 patients altogether, 8 of whom had long QT syndrome. Of the 12 non–long QT patients, 6 were female, 4 had an old myocardial infarction, and 3 were taking a class I AAD. Short episodes of TdP were repeatedly observed before the cardiac arrest.

In the 37 survivors, the fatal VTAs converted to a basic rhythm with resuscitation in 13 patients (35%) or spontaneously in 24 patients (65%). Any symptoms were documented in 23 patients (62%), which included syncope or faintness in 83%, chest pain in 22%, and convulsion in 4% (with duplication). Twelve patients who did not claim any symptoms had spontaneous conversions during the night. In addition, the survivors had 3.8 ± 5.6 preceding VTA episodes.

A multivariate logistic regression analysis revealed that the independent predictors of mortality were age (OR 1.04, 95% confidence interval [CI] 1.02–1.08, $P < .001$), and preceding ST elevation (OR 3.54, 95% CI 1.07–13.5, $P = .039$). In contrast, the presence of preceding TdP was associated with a better survival (OR 0.20, 95% CI 0.05–0.66, $P = .011$).

Bradyarrhythmia patients

Baseline characteristics, preceding electrical events, and outcomes in the bradyarrhythmia patients are presented in Online Supplemental Tables 1 and 2. The mortality rate was higher in the patients with asystole than in those with AV block (Figure 1B).

Table 2 Baseline characteristics of the ventricular tachyarrhythmia patients

	VT/VF (n = 59)	Primary VF (n = 23)	TdP (n = 10)	VT (n = 5)	*P* value
Age (years)	57 ± 19	62 ± 15	53 ± 16	54 ± 16	.430
Male [n (%)]	34 (58)	20 (87)	4 (40)	3 (60)	.034
Basic rhythm [n (%)]					
Sinus rhythm	55 (93)	21 (91)	9 (90)	5 (100)	.897
AF	4 (7)	0 (0)	1 (10)	0 (0)	.510
Complete AV block	0 (0)	2 (9)	0 (0)	0 (0)	.086
Underlying disease [n (%)]					
Acute coronary syndrome	3 (5)	2 (9)	0 (0)	0 (0)	<.001
Old myocardial infarction	12 (20)	4 (17)	0 (0)	2 (40)	.268
Effort angina	13 (22)	7 (30)	1 (10)	2 (40)	.486
Vasospastic angina	2 (3)	0 (0)	0 (0)	0 (0)	.725
Hypertension	2 (3)	0 (0)	3 (30)	1 (20)	.038
Dilated cardiomyopathy	9 (15)	0 (0)	0 (0)	0 (0)	.094
Long QT syndrome	3 (5)	1 (4)	4 (40)	0 (0)	.002
Brugada syndrome	1 (2)	0 (0)	1 (10)	0 (0)	.289
Valvular heart disease	1 (2)	0 (0)	0 (0)	0 (0)	.885
Heart failure	4 (7)	3 (13)	0 (0)	1 (20)	.443
Stroke	3 (5)	0 (0)	2 (20)	0 (0)	.110
Preceding electrical events [n (%)]					
Tachycardia	17 (29)	2 (9)	0 (0)	1 (20)	.071
Bradycardia	2 (3)	3 (13)	0 (0)	0 (0)	.248
Premature atrial complex	5 (8)	3 (13)	1 (10)	1 (20)	.823
Premature ventricular complex	25 (42)	11 (48)	1 (10)	2 (40)	.210
Nonsustained VT	20 (34)	2 (9)	1 (10)	1 (20)	.069
Torsades de pointes	9 (15)	2 (9)	9 (90)	1 (20)	<.001
R-on-T phenomenon	46 (78)	16 (70)	6 (60)	1 (20)	.016
T-wave alternans	1 (2)	0 (0)	0 (0)	0 (0)	.726
Paroxysmal AF	5 (8)	3 (13)	1 (10)	0 (0)	.813
ST elevation	15 (25)	8 (35)	2 (20)	1 (20)	.763
ST depression	20 (34)	7 (30)	2 (20)	0 (0)	.383
Therapy [n (%)]					
Beta-blocker	5 (8)	2 (9)	2 (20)	1 (20)	.614
Class I AAD	11 (19)	0 (0)	3 (33)	2 (40)	.044
Class III AAD	0 (0)	2 (9)	0 (0)	1 (20)	.614
ICD implantation	1 (2)	0 (0)	0 (0)	0 (0)	.885

Data are given as mean ± SD or number (frequency).
AAD = antiarrhythmic drug; AF = atrial fibrillation; AV = atrioventricular; ICD = implantable cardioverter-defibrillator; VF = ventricular fibrillation; VT = ventricular tachycardia.

Circadian variation

The distribution of the frequency of SCAs is shown in Figure 2. The fast Fourier transform failed to detect any significant peak of the onset of SCA when applied to the data from all patients ($P = .965$; Figure 2A), survivors ($P = .756$), or nonsurvivors ($P = .807$), VTA ($P = .896$; Figure 2B), or bradyarrhythmia ($P = .357$; Figure 2C), and an ischemic etiology ($P = .944$) or nonischemic etiology ($P = .957$). Of note, the patients with Brugada syndrome (n = 2; 11:32 PM and 5:13 AM) and vasospastic angina (n = 4; 2:31 AM, 3:41 AM, 4:55 AM, and 5:39 AM) had SCA events from night to early morning.

Discussion

Major findings

In patients who had SCA during Holter recording, 73% of the SCAs resulted from VTAs, similar to the previous studies.[8,13,15,18] The novel findings of the current study were that advanced age and ST elevation the hour before SCA were independent predictors of mortality. We observed that approximately 40% of patients with VTAs experienced self-termination of the arrhythmias with either cardiopulmonary resuscitation or spontaneously. Furthermore, we found that TdP, observed as a premonitory event, was associated with spontaneous conversion. Bradyarrhythmia-related SCAs were characterized by advanced age and higher frequency of comorbidities compared to patients with VTA-related SCAs.

Mechanism of SCA

Our study showed that 73% of SCAs resulted from VTAs that included VT degenerating to VF (45%), followed by primary VF (17%), TdP (7%), and VT throughout the arrest (4%). Bayes de Luna et al[8] demonstrated that the most frequent causes of SCA were VT degenerating to VF (62.4%), followed by TdP (12.7%) and primary VF (8.3%). The proportion of the VTAs in our study was similar to their data; however, the incidence of primary VF was double that of their study.

In an earlier study, ischemic ST changes prior to fatal arrhythmias were found in 12.6%,[8] but our data showed that ST elevation or ST depression was observed in 28% and

Table 3 Baseline characteristics and preceding events in ventricular tachyarrhythmia patients classified according to outcome

	Nonsurvivors (n = 60)	Survivors (n = 37)	*P* value
Age (years)	64 ± 17	48 ± 18	<.001
Male [n (%)]	42 (70)	19 (51)	.064
Basic rhythm [n (%)]			
Sinus rhythm	53 (89)	37 (100)	.031
AF	5 (8)	0 (0)	.183
Complete AV block	2 (3)	0 (0)	.380
Underlying disease [n (%)]			
Acute coronary syndrome	2 (3)	3 (8)	.281
Old myocardial infarction	13 (22)	5 (14)	.233
Effort angina	17 (28)	6 (16)	.131
Vasospastic angina	0 (0)	2 (5)	.143
Hypertension	3 (5)	3 (8)	.416
Dilated cardiomyopathy	7 (12)	2 (5)	.256
Long QT syndrome	1 (2)	7 (19)	.004
Brugada syndrome	0 (0)	2 (5)	.138
Valvular heart disease	1 (2)	0 (0)	.143
Heart failure	8 (13)	0 (0)	.018
Stroke	3 (5)	2 (5)	.635
Preceding electrical events [n (%)]			
Tachycardia	16 (27)	4 (11)	.049
Bradycardia	5 (8)	0 (0)	.085
Premature atrial complex	7 (12)	3 (8)	.423
Premature ventricular complex	23 (38)	16 (43)	.394
Nonsustained VT	12 (20)	12 (32)	.128
Torsades de pointes	4 (7)	16 (43)	<.001
R-on-T phenomenon	42 (70)	27 (73)	.754
T-wave alternans	0 (0)	1 (3)	.381
Paroxysmal AF	5 (8)	4 (11)	.471
ST elevation	21 (35)	5 (14)	.016
ST depression	21 (35)	8 (22)	.120
Therapy [n (%)]			
Beta-blocker	4 (7)	6 (17)	.124
Class I AAD	11 (18)	5 (14)	.372
Class III AAD	2 (3)	1 (3)	.676
ICD implantation	0 (0)	1 (3)	.381

Data are given as mean ± SD or number (frequency).
AAD = antiarrhythmic drug; AF = atrial fibrillation; AV = atrioventricular; ICD = implantable cardioverter-defibrillator; VF = ventricular fibrillation; VT = ventricular tachycardia.

33%, respectively, prior to the onset of SCAs from VTAs. Multivariate logistic regression analysis revealed that ST elevation was an independent predictor of death with VTAs, suggesting that myocardial ischemia may play a role in VTAs followed by SCA. The preceding ischemic ECG sign and VTAs would have an impact on the management of SCA.

Spontaneous conversion of VTAs

We found that approximately 40% of the patients with VTAs had a spontaneous conversion, of whom 35% of patients required cardiopulmonary resuscitation and 65% had spontaneously restored basic rhythm. Nearly 60% of the survivors experienced symptoms, but the remaining patients did not claim symptoms, probably because spontaneous conversion occurred during sleeping hours.

Spontaneous conversion was observed in young patients who had no structural heart disease, which is consistent with previous reports.[24,25] TdP was often associated with spontaneous conversion to sinus rhythm not only in long QT syndrome but also in cases with an old myocardial infarction. It occurred more frequently in females and in patients receiving class I AAD therapy.[26] Because spontaneous conversion must happen by chance, we cannot expect the same phenomena in the subsequent episode of VF.

The mechanisms of self-termination of TdP or VF may involve hyperkalemia or an elevation of the released catecholamines as shown in animal experiments.[27,28] However, this hypothesis is based on animal studies showing that transient VF is a normal feature in mammals that have predominantly sympathetic autoregulation. Understanding the mechanisms of spontaneous conversion may provide therapeutic options.

Bradyarrhythmia-related SCA

Our data showed that the frequency of bradyarrhythmia-related SCAs was 27%, which was higher than the 16% reported by Bayes de Luna et al.[8] We found that there was a higher frequency of coexisting strokes and heart failure, which was consistent with previous studies.[19,29–31]

Circadian pattern of SCA

Multiple studies reported a significant circadian periodicity at the time of onset of an acute myocardial infarction or sudden death, with a peak incidence in the morning hours.[32] For the peak incidence of such acute cardiovascular events in the morning, enhanced sympathetic activity, a "sympathetic morning surge," is believed to play a main role.[26,32] However, we could not delineate any rhythmicity in SCA in the present study. This observation may be related to the effect of medications, or the background of the patients who underwent Holter recording might have differed from the subjects in the general population.

Study limitations

This study was retrospective and was not based on the general population but on patients who required Holter recording for medical reasons. The race or the physical and emotional activities before SCA were not assessed.[33,34] It is important and instructive to examine the frequency of SCAs during Holter recordings. Unfortunately, we did not include this investigation item in the study protocol; thus, we were not able to assess the SCA occurrence rate. This SCA occurrence rate may vary according to the characteristics of the institution and/or the severity of condition in the patients.

Conclusion

We showed that the major mechanism of SCA was VTAs. In the VTAs, self-termination was observed, especially in

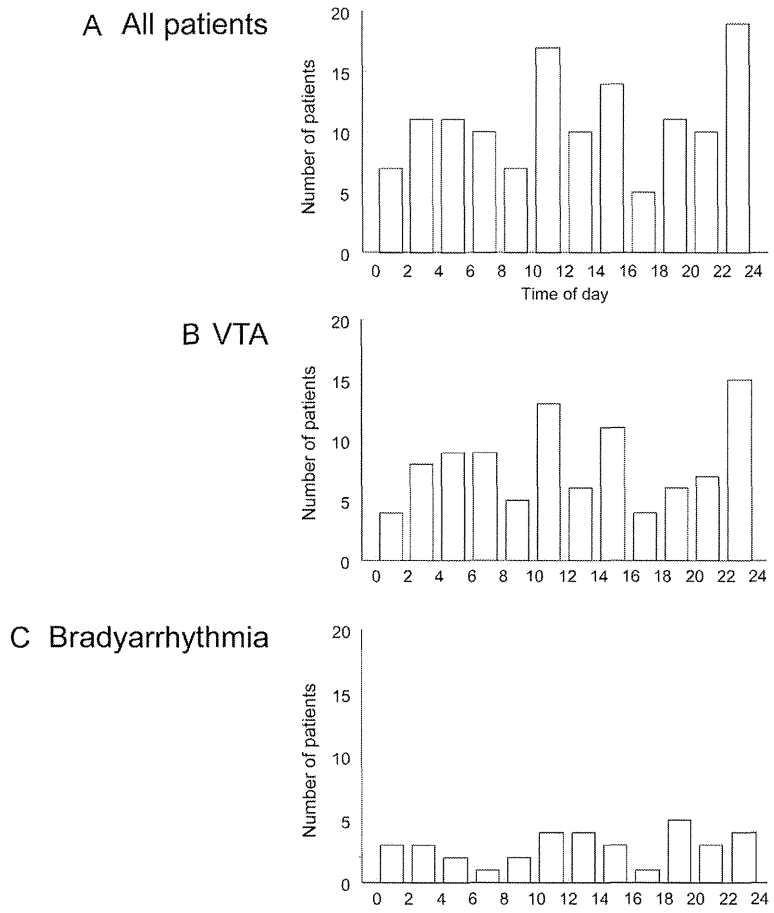

Figure 2 Distribution of sudden cardiac arrest. **A:** All patients. **B:** Ventricular tachyarrhythmia (VTA). **C:** Bradyarrhythmia. Fast Fourier transformation failed to detect any significant peaks of the onset (A) through (C).

patients who were young and had no structural heart disease. Advanced age and ST elevation the hour before SCA were independent predictors of mortality for the VTAs. TdP, observed as a premonitory event, was associated with spontaneous conversion. The patients with bradyarrhythmia-related SCAs were older and characterized by a higher frequency of comorbidities.

Acknowledgments

The following persons participated in this study: Naohiko Tashiro, Naka Sakamoto, Toshiharu Takeuchi, Yasuko Tanabe, Nobuyuki Sato, Yuichirou Kawamura, Naoyuki Hasebe, Akira Kondo, Naoki Chiba, Seizo Oriso, Naohiko Takahashi, Tetsuji Shinohara, Tetsunori Saikawa, Hisaaki Morita, Hirohide Matsuo, Koushi Mawatari, Makoto Suzuki, Yoshiaki Yokoi, Yoshihiro Yumoto, Shinichi Niwano, Shinichi Hirano, Keita Odashiro, Akiko Chishaki, Toru Maruyama, Kenichi Hiasa, Kenji Sunagawa, Yukiko Nishio, Daisuke Inoue, Keizo Mahara, Akihiro Tanabe, Kenji Takagaki, Katsuro Shimomura, Tatsuya Wada, Yoshikazu Hiasa, Minoru Horie, Yoshihiko Miyake, Tadakazu Sato, Satoru Kobayashi, Toshihiro Sato, Hiroshi Maeda, Iwao Yamaguchi, Teruhisa Tanabe, Makiyoshi Shima, Mari Amino, Koichiro Yoshioka, Keiko Oikawa, Norishige Morita, Yoshinori Kobayashi, Toru Sawanobori, Masayasu Hiraoka, Fumiko Tomimatsu, Hiroshi Inoue, Kaoru Sugi, Shingo Kujime, Mahito Noro, Kan Takayanagi, Atsushi Okamura, Yukihiro Fujimoto, Akira Fujiki, Toshio Torii, Shojiro Isomoto, Masahiko Fukaya, Rinya Kato, Masaya Shimizu, Jun Ochiai, Aiko Fujimoto, Yoshifusa Aizawa, Katsuya Ebe, Yasushi Miyauchi, Takao Kato, Kyoichi Mizuno, Motohisa Osaka, Mitsunori Maruyama, Reiko Okazaki, Hiroshige Murata, Ichiro Watanabe, Satoshi Saito, Junji Fukuhara, Hiroshi Kanamaru, Naokata Sumitomo, Susumu Nagasawa, Kazuo Moroe, Hitoshi Chikamatsu, Makoto Nonogawa, Nobuko Kodama, Masato Iida, Bonpei Takase, Kan Hara, Takakazu Kato, Akira Hamabe, Issei Kimura, Hiroshi Arakawa, Masatoshi Kusuhara, Fumitaka Ohsuzu, Akimi Uehata, Masayuki Ishihara, Takuya Mori, Tokuji Konishi, Koichi Yokoyama, Tetsu Watanabe, Joji Nitobe, Isao Kubota, Motoyuki Matsui, Kozue Ikeda, Yuzo Shimizu, Shunichi Kaseda, Mikio Arita, Kazuya Fukuda, Chuichi Sato, Yoshio Nakamura, Ken Okumura, Hirotsugu

Atarashi, Itsuo Kodama, Eiichi Watanabe, Tsuneaki Sugimoto, and Yoshio Watanabe. The authors thank Ms. Akemi Yamauchi for preparing the manuscript.

Appendix

Supplementary data

Supplementary data associated with this article can be found in the online version at http://dx.doi.org/10.1016/j.hrthm.2014.04.036.

References

1. Zipes DP, Camm AJ, Borggrefe M, et al. ACC/AHA/ESC 2006 guidelines for management of patients with ventricular arrhythmias and the prevention of sudden cardiac death: a report of the American College of Cardiology/American Heart Association Task Force and the European Society of Cardiology Committee for Practice Guidelines. J Am Coll Cardiol 2006;48:e247–e346.
2. Deo R, Albert CM. Epidemiology and genetics of sudden cardiac death. Circulation 2012;125:620–637.
3. Chugh SS, Jui J, Gunson K, et al. Current burden of sudden cardiac death: multiple source surveillance versus retrospective death certificate-based review in a large U.S. community. J Am Coll Cardiol 2004;44:1268–1275.
4. Nichol G, Thomas E, Callaway CW, et al. Regional variation in out-of-hospital cardiac arrest incidence and outcome. JAMA 2008;300:1423–1431.
5. Kong MH, Fonarow GC, Peterson ED, Curtis AB, Hernandez AF, Sanders GD, Thomas KL, Hayes DL, Al-Khatib SM. Systematic review of the incidence of sudden cardiac death in the United States. J Am Coll Cardiol 2011;57:794–801.
6. Statistics of sudden cardiac arrest in Japan. http://www.fdma.go.jp/html/hakusho/h24/h24/html/2-2-5-5_2.html?words.
7. Kitamura T, Iwami T, Kawamura T, Nitta M, Nagao K, Nonogi H, Yonemoto N, Kimura T, for the Japanese Circulation Society Resuscitation Science Study G. Nationwide improvements in survival from out-of-hospital cardiac arrest in Japan. Circulation 2012;126:2834–2843.
8. Bayes de Luna A, Coumel P, Leclercq JF. Ambulatory sudden cardiac death: mechanisms of production of fatal arrhythmia on the basis of data from 157 cases. Am Heart J 1989;117:151–159.
9. Herlitz J, Andersson E, Bang A, Engdahl J, Holmberg M, lindqvist J, Karlson BW, Waagstein L. Experiences from treatment of out-of-hospital cardiac arrest during 17 years in Goteborg. Eur Heart J 2000;21:1251–1258.
10. Cobb LA, Fahrenbruch CE, Olsufka M, Copass MK. Changing incidence of out-of-hospital ventricular fibrillation, 1980-2000. JAMA 2002;288:3008–3013.
11. Go AS, Mozaffarian D, Roger VL, et al. Heart disease and stroke statistics—2013 update: a report from the American Heart Association. Circulation 2013;127:e6–e245.
12. Kuisma M, Repo J, Alaspaa A. The incidence of out-of-hospital ventricular fibrillation in Helsinki, Finland, from 1994 to 1999. Lancet 2001;358:473–474.
13. Kempf FC Jr, Josephson ME. Cardiac arrest recorded on ambulatory electrocardiograms. Am J Cardiol 1984;53:1577–1582.
14. Pratt CM, Francis MJ, Luck JC, Wyndham CR, Miller RR, Quinones MA. Analysis of ambulatory electrocardiograms in 15 patients during spontaneous ventricular fibrillation with special reference to preceding arrhythmic events. J Am Coll Cardiol 1983;2:789–797.
15. Milner PG, Platia EV, Reid PR, Griffith LS. Ambulatory electrocardiographic recordings at the time of fatal cardiac arrest. Am J Cardiol 1985;56:588–592.
16. Lewis BH, Antman EM, Graboys TB. Detailed analysis of 24 hour ambulatory electrocardiographic recordings during ventricular fibrillation or torsade de pointes. J Am Coll Cardiol 1983;2:426–436.
17. Roelandt J, Klootwijk P, Lubsen J, Janse MJ. Sudden death during longterm ambulatory monitoring. Eur Heart J 1984;5:7–20.
18. Panidis IP, Morganroth J. Sudden death in hospitalized patients: cardiac rhythm disturbances detected by ambulatory electrocardiographic monitoring. J Am Coll Cardiol 1983;2:798–805.
19. Wang FS, Lien WP, Fong TE, Lin JL, Cherng JJ, Chen JH, Chen JJ. Terminal cardiac electrical activity in adults who die without apparent cardiac disease. Am J Cardiol 1986;58:491–495.
20. Yagi S. Proceedings of the meeting for case studies of sudden death during Holter ECG recording. Tokyo Excerpta Medica (in Japanese). 1991.
21. Tanabe T. Proceedings of the meeting for case studies of sudden death during Holter ECG recording. Hadano: Tokai University Press (in Japanese). 2010.
22. Osaka M, Watanabe E, Murata H, Fuwamoto Y, Nanba S, Sakai K, Katoh T. V-shaped trough in autonomic activity is a possible precursor of life-threatening cardiac events. Circ J 2010;74:1906–1915.
23. Wu MC, Watanabe E, Struzik ZR, Hu CK, Yamamoto Y. Phase statistics approach to human ventricular fibrillation. Phys Rev E 2009;80:051917.
24. van Hemel NM, Kingma JH. A patient in whom self-terminating ventricular fibrillation was a manifestation of myocardial reperfusion. Br Heart J 1993;69:568–571.
25. Nair K, Umapathy K, Downar E, Nanthakumar K. Aborted sudden death from sustained ventricular fibrillation. Heart Rhythm 2008;5:1198–1200.
26. Kong TQ Jr, Goldberger JJ, Parker M, Wang T, Kadish AH. Circadian variation in human ventricular refractoriness. Circulation 1995;92:1507–1516.
27. Reisin L, Blayer Y, Manoach M. Spontaneous ventricular defibrillation. Br Heart J 1993;70:590–591.
28. Pandit SV, Warren M, Mironov S, Tolkacheva EG, Kalifa J, Berenfeld O, Jalife J. Mechanisms underlying the antifibrillatory action of hyperkalemia in Guinea pig hearts. Biophys J 2010;98:2091–2101.
29. Luu M, Stevenson WG, Stevenson LW, Baron K, Walden J. Diverse mechanisms of unexpected cardiac arrest in advanced heart failure. Circulation 1989;80:1675–1680.
30. Tokgozoglu SL, Batur MK, Top uoglu MA, Saribas O, Kes S, Oto A. Effects of stroke localization on cardiac autonomic balance and sudden death. Stroke 1999;30:1307–1311.
31. Oppenheimer S. Cerebrogenic cardiac arrhythmias: cortical lateralization and clinical significance. Clin Auton Res 2006;16:6–11.
32. Muller JE, Stone PH, Turi ZG, Rutherford JD, Czeisler CA, Parker C, Poole WK, Passamani E, Roberts R, Robertson T, et al. Circadian variation in the frequency of onset of acute myocardial infarction. N Engl J Med 1985;313:1315–1322.
33. Chugh SS, Reinier K, Teodorescu C, Evanado A, Kehr E, Al Samara M, Mariani R, Gunson K, Jui J. Epidemiology of sudden cardiac death: clinical and research implications. Prog Cardiovasc Dis 2008;51:213–228.
34. Reddy PR, Reinier K, Singh T, Mariani R, Gunson K, Jui J, Chugh SS. Physical activity as a trigger of sudden cardiac arrest: the Oregon Sudden Unexpected Death Study. Int J Cardiol 2009;131:345–349.

Biochemical and Biophysical Research Communications 452 (2014) 701–707

Contents lists available at ScienceDirect

Biochemical and Biophysical Research Communications

journal homepage: www.elsevier.com/locate/ybbrc

Suppression of Rad leads to arrhythmogenesis via PKA-mediated phosphorylation of ryanodine receptor activity in the heart

Hiroyuki Yamakawa [a], Mitsushige Murata [b,*], Tomoyuki Suzuki [c], Hirotaka Yada [d], Hideyuki Ishida [e], Yoshiyasu Aizawa [a], Takeshi Adachi [d], Kaichiro Kamiya [c], Keiichi Fukuda [a]

[a] Department of Cardiology, School of Medicine, Keio University, Tokyo, Japan
[b] Department of Laboratory Medicine, School of Medicine, Keio University, Tokyo, Japan
[c] Department of Cardiovascular Research, Research Institute of Environmental Medicine, Nagoya University, Nagoya, Japan
[d] Department of Cardiology, First Internal Medicine, National Defense Medical College, Saitama, Japan
[e] Department of Physiology, Tokai University School of Medicine, Kanagawa, Japan

ARTICLE INFO

Article history:
Received 18 August 2014
Available online 1 September 2014

Keywords:
Rad (Ras associated with diabetes)
Excitation–contraction (EC) coupling (ECC)
Ryanodine receptor
Ca^{2+} imaging
PKA signaling

ABSTRACT

Ras-related small G-protein Rad plays a critical role in generating arrhythmias via regulation of the L-type Ca^{2+} channel (LTCC). The aim was to demonstrate the role of Rad in intracellular calcium homeostasis by cardiac-Specific dominant-negative suppression of Rad. Transgenic (TG) mice overexpressing dominant-negative mutant Rad (S105N Rad TG) were generated. To measure intracellular Ca^{2+} concentration ($[Ca^{2+}]_i$), we recorded $[Ca^{2+}]_i$ transients and Ca^{2+} sparks from isolated cardiomyocytes using confocal microscopy. The mean $[Ca^{2+}]_i$ transient amplitude was significantly increased in S105N Rad TG cardiomyocytes, compared with control littermate mouse cells. The frequency of Ca^{2+} sparks was also significantly higher in TG cells than in control cells, although there were no significant differences in amplitude. The sarcoplasmic reticulum Ca^{2+} content was not altered in the S105N Rad TG cells, as assessed by measuring caffeine-induced $[Ca^{2+}]_i$ transient. In contrast, phosphorylation of Ser^{2809} on the cardiac ryanodine receptor (RyR2) was significantly enhanced in TG mouse hearts compared with controls. Additionally, the Rad-mediated RyR2 phosphorylation was regulated via a direct interaction of Rad with protein kinase A (PKA).

1. Introduction

Rad (Ras associated with diabetes) is a member of the Ras-related Rad, Gem, and Kir (RGK) family of small GTP binding proteins, which was identified by subtractive cloning as overexpressed in skeletal muscle of patients with type 2 diabetes mellitus [1,2]. The RGK family encodes GTP-binding proteins with several structural features that are distinct from other GTPases [3,4]. Compared to Ras, the N-terminus of Rad is extended by 88 amino acids and the C-terminus is extended by 31 amino acids, and Rad lacks a CAAX-like prenylation site present in other Ras-like molecules [5,6]. These characteristic structures allow Rad to interact with a variety of cellular effectors to participate in many biological functions. Rad can inhibit insulin-stimulated glucose uptake in myocyte and adipocyte cell lines [6] and regulate neurite extension via Rho/RhoA kinase (ROK) signaling [7], and Rad expression is upregulated in vascular smooth muscle cells (VSMCs) during vascular lesion formation [8]. Regarding the role of Rad in the heart, we previously reported that Rad could function as a potent inhibitor of voltage-dependent calcium channels by directly binding to their β-subunit and that dominant-negative suppression of Rad induced ventricular arrhythmias [9]. Other groups have also reported the physiological importance of Rad in cardiac functions [9–11]. Chang et al. reported that Rad is downregulated in the human failing heart and knocking out Rad in mouse heart exaggerated cardiac hypertrophic remodeling under pressure overload conditions, via enhanced Ca^{2+}/calmodulin-dependent kinase II (CaMKII) signaling [10]. Rad also serves as an important endogenous regulator of cardiac excitation–contraction (EC) coupling and β-adrenergic signaling [11]. Together, these results including our study indicate that Rad may interact with a signaling pathway that regulates Ca^{2+} homeostasis in cardiomyocytes, which may in turn influence arrhythmias as well as the remodeling of hypertrophy in hearts. However, the mechanism for Rad-mediated regulation of intracellular Ca^{2+} homeostasis in cardiomyocytes has not been fully elucidated.

* Corresponding author. Address: Department of Laboratory Medicine, Keio University, 35 Shinanomachi, Shinjuku-ku, Tokyo 160-8582, Japan. Fax: +81 3 5363 3875.
E-mail address: muratam@a7.keio.jp (M. Murata).

http://dx.doi.org/10.1016/j.bbrc.2014.08.126
0006-291X/

The main goal of this study was therefore to examine the effect of Rad on cardiac intracellular calcium homeostasis and to clarify its mechanisms using an *in vivo* mouse model of cardiac-specific dominant-negative suppression of Rad.

2. Methods

All experimental procedures and protocols were approved by the Animal Care and Use Committee of Keio University (20-041-4) and conformed to the NIH Guide for the Care and Use of Laboratory Animals (NIH Publication No. 85-23 revised 1996).

2.1. Adenoviral transduction and cell culture

Ventricular cardiomyocytes were isolated from the left ventricles of adult mice using enzymatic digestions as previously described, with slight modifications [9]. Isolated cardiomyocytes were re-suspended in Dulbecco's modified Eagle's medium (DMEM) containing 10% fetal bovine serum (FBS) and 1% penicillin–streptomycin (all from Invitrogen, Carlsbad, CA) and then plated at a density of 6×10^5/dish. Adenovirus harboring Ad-GFP and Ad-S105N Rad was added to the culture medium of cardiomyocytes. Cultured cardiomyocytes of Ad-GFP and Ad-S105N Rad were utilized as electrophysiological and biochemical measurements 24 h after infection.

2.2. Electrophysiological experiments

The L-type calcium current ($I_{Ca,L}$) and action potential were recorded using the whole-cell patch clamp technique with an Axopatch 200B amplifier (Axon Instruments, Foster City, CA). All recordings from myocytes were performed at 37 °C. Cells were superfused in solution containing (in mmol/L) 140 NaCl, 5 KCl, 1 $MgCl_2$, 10 HEPES, 2 $CaCl_2$, and 10 glucose (pH 7.4, adjusted with NaOH). For $I_{Ca,L}$ recordings, the external solution was replaced with a Na^+, K^+-free solution after establishing the whole-cell clamp mode. The micropipette electrode solution for measuring $I_{Ca,L}$ was composed of (in mmol/L) 60 CsOH, 80 CsCl, 40 asparate, 5 HEPES, 10 EGTA, 5 MgATP, 5 phosphocreatinine, and 0.65 $CaCl_2$. L-type calcium currents were elicited by 300-ms depolarizing steps from −40 to 65 mV, in 5-mV increments.

Action potentials (APs) were recorded in an external solution containing (in mmol/L) 140 NaCl, 5 KCl, 1 $MgCl_2$, 10 HEPES, 1.8 $CaCl_2$, and 10 glucose (pH 7.4, adjusted with NaOH). The micropipette electrode solution for recording action potentials was composed of (in mmol/L) 130 K-glutamate, 9 KCl, 10 HEPES, 2 EGTA, and 5 MgATP (pH 7.2, adjusted with KOH). Action potentials were initiated by short depolarizing current pulses (2–3 ms, 500–800 pA) at 2 Hz. Ba^{2+} currents were recorded at 25 °C in an external solution containing (in mmol/L) NaCl 140, CsCl 5, $BaCl_2$ 4, $MgCl_2$ 1.0, glucose 10, and HEPES 10 (pH 7.4, adjusted with NaOH).

2.3. Calcium imaging experiments

Initially, myocytes were loaded at 37 °C with Fluo-4 AM (10 μM; Molecular Probes) for 30 min to measure $[Ca^{2+}]_i$ transient, Ca^{2+} spark, and Ca^{2+} wave. The cells were then assessed for Fluo-4 fluorescent signal intensity at room temperature using a Zeiss LSM-510 confocal microscope (5-Live mode) with a × 40 lens (NA 1.3) and laser excitation/emission (488/543 nm) [12]. Myocytes were incubated in 1.0 mM Ca^{2+} Tyrode solution and stimulated via platinum electrodes connected to a stimulator at a frequency of 1 Hz. Contraction amplitudes and rates of contraction and relaxation were recorded online with a video edge-detection system and data acquisition software as described previously [12]. The sarcoplasmic reticulum (SR) Ca^{2+} content was evaluated after rapid injection of caffeine (10 mM) [13] and expressed as a relative value of the baseline value, F/F_0.

2.4. Western blotting

Total protein was extracted from frozen hearts. Equal amounts of total extracted protein (20–50 μg) were subjected to SDS–PAGE. A rabbit anti-Rad polyclonal antibody (a kind gift from Ronald Kahn in the Joslin Diabetes Center, Harvard Medical School) was used for Rad detection. The other primary antibodies were purchased as follows: anti-cardiac Ca^{2+} ATPase (SERCA2a), anti-phospholamban (PLB), and anti-phospho-PLB Ser^{16} (p-PLB Ser^{16}) (Affinity BioReagents); anti-Na^+/Ca^{2+} exchanger (NCX) (Abcam); anti-RyR2, anti-phospho-RyR Ser^{2809} (p-RyR Ser^{2809}), anti-PKA-C (PKA catalytic subunit), and anti-phospho-PKA C Thr^{197} (p-PKA C Thr^{197}) (Cell Signaling Technology); anti-β1 AR and anti-β2 AR (Sigma–Aldrich).

2.5. PKA kinase assay

The samples of heart tissues (about each 10 g) were homogenized in 1 ml of 0.1 N HCl. The lysates were centrifuged at 1200*g* for 10 min at 4°. The supernatants were assayed immediately. The concentrations of cAMP were measured using a radioimmunoassay kit (Yamasa).

2.6. Statistical analysis

All data are shown as mean ± SEM. Statistical differences were determined using repeated-measures ANOVA, and $P < 0.05$ was considered significant.

3. Results

3.1. Dominant-negative suppression of Rad in cardiomyocytes leads to the induction of triggered activities

To first confirm the dominant-negative Rad effect on $I_{Ca,L}$ in genetically modified mouse cells, we measured $I_{Ca,L}$ from wild-type littermates (control) and S105N Rad TG mouse cardiomyocytes using whole-cell patch clamping in voltage clamp mode. Fig. 1A shows representative $I_{Ca,L}$ traces recorded from control and S105N Rad TG cardiomyocytes. The peak $I_{Ca,L}$ was dramatically larger in the S105N Rad TG cells than in controls (15.9 ± 1.0 pA/pF at 5 mV ($n = 4$) in S105N Rad vs 9.4 ± 0.9 pA/pF at 5 mV ($n = 8$) in control, Fig. 1A). In contrast, there were no significant differences in steady-state inactivation curves ($n = 7$) and activation curves ($n = 8$) between these groups (Fig. 1B).

Next, we recorded the action potentials (APs) in current-clamp mode. Fig. 1C shows representative AP traces from control and S105N Rad TG cells. Both AP durations were significantly prolonged at 50% repolarization (APD_{50}) and at 90% (APD_{90}) in S105N Rad TG cells, compared with control cells (APD_{90}: 53.2 ± 7.3 ms ($n = 4$) in S105N Rad vs 30.8 ± 4.6 ms ($n = 7$) in control, Fig. 1D). Consistent with the prolongation of APDs in S105N Rad TG cells, the abnormal potentials like triggered activities including delayed after depolarizations (DADs) and early after depolarizations (EADs) were observed in S105N Rad TG cells (Fig. 1E), while no abnormal activities were observed in controls, implicating the intracellular Ca^{2+} overload by downregulation of Rad activity.

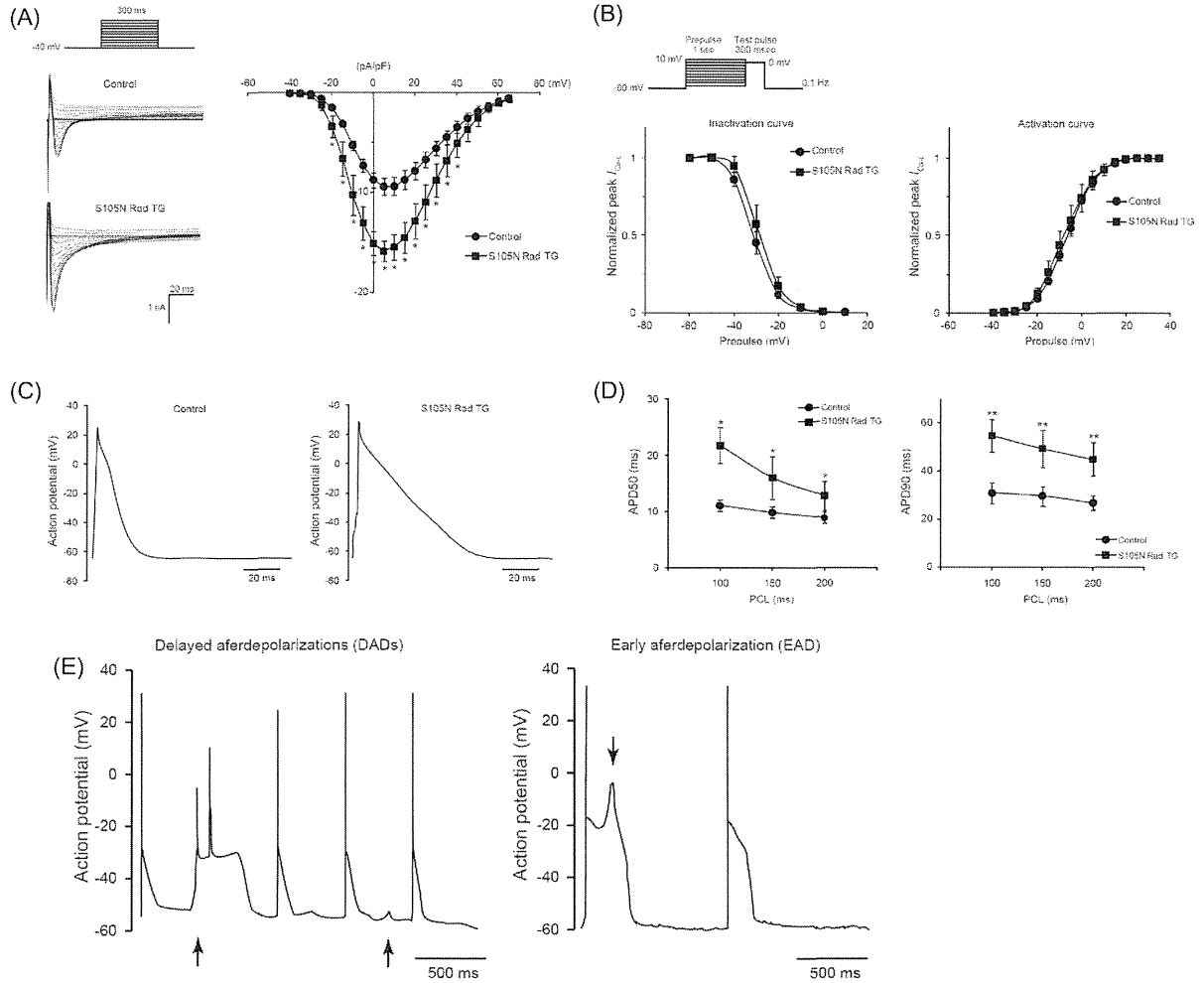

Fig. 1. The electrophysiological properties in S105N Rad TG mice. (A) Representative $I_{Ca,L}$ in control and dominant negative Rad (S105N Rad) TG mouse (left panel). The peak $I_{Ca,L}$ was dramatically larger in the S105N Rad TG cells than in controls (right panel -15.9 ± 1.0 pA/pF at 5 mV ($n = 4$) in S105N Rad vs -9.4 ± 0.9 pA/pF at 5 mV ($n = 8$) in control; $P < 0.01$). (B) The effect of Rad activity on activation and inactivation curves in $I_{Ca,L}$ (inactivation curves (left panel) and activation curves (left panel)). There were no significant differences in steady-state inactivation curves among these groups ($n = 7$) and in steady-state inactivation curves among these groups ($n = 8$). (C) Representative action potential traces recorded from control and S105N Rad TG mouse cardiomyocytes. (D) Action potential duration at 50% repolarization (APD_{50}) and at 90% (APD_{90}). APD_{50} in S105N Rad TG was significantly prolonged compared with control cells (APD_{50} at the pacing length of 100 ms: 21.7 ± 3.2 ms ($n = 7$) in S105N Rad cells vs 11.1 ± 1.6 ms ($n = 7$) in controls; $P = 0.02$). APD_{90} in S105N Rad TG was significantly prolonged compared with control cells (APD_{90} at the pacing length of 100 ms: 54.7 ± 6.8 ms ($n = 7$) in S105N Rad cells vs 30.8 ± 4.6 ms ($n = 7$) in controls; $P = 0.04$). (E) Triggered activities in S105N Rad. Delayed afterdepolarization (DAD) was observed in S105N Rad TG mouse (left panel). Early afterdepolarization (EAD) was also observed in S105N Rad (right panel). However, no abnormal activities were observed in control cells.

3.2. Rad regulates intracellular Ca^{2+} homeostasis in cardiomyocytes

To evaluate Ca^{2+} overload in S105N Rad TG mice, we investigated the effects of Rad on intracellular Ca^{2+} concentration using Ca^{2+} indicator, Fluo-4 AM. Fig. 2A and B show the representative line scan images, and their corresponding $[Ca^{2+}]_i$ transients by field stimulation at 1 Hz in cardiomyocytes obtained from control and S105N Rad TG mice. The amplitude of $[Ca^{2+}]_i$ transients (F/F_0) was larger in S105N Rad TG cell than in controls, showing a mean increase of 34%. In contrast, there were no significant differences in decreased time to 50% relaxation (RT50) or the tendency for a decrease of the time constant (τ of $[Ca^{2+}]_i$ decline in cardiomyocytes, which was indicated as the index of relaxation (Fig. 2C). A possible mechanism for the effect of Rad on the $[Ca^{2+}]_i$ transient amplitudes could involve the regulation of SR Ca^{2+} content. To clarify this possibility, we measured caffeine-evoked $[Ca^{2+}]_i$ transients; however, there were no significant differences in the amplitude, τ, or RT50 of $[Ca^{2+}]_i$ transients between S105N Rad TG and control cells (Fig. 2D).

The spatial and temporal uniformity of Ca^{2+} transients are important aspects of cardiac EC coupling and its modulation by β-AR stimulation [14]. In heart failure models, dis-synchronous SR Ca^{2+} releases, such as Ca^{2+} sparks and waves, have also been linked to reduced inotropy and enhanced arrhythmogenesis [15]. To investigate the Ca^{2+} leak in S105N Rad TG mice, we therefore recorded Ca^{2+} sparks emitted from isolated S105N Rad TG and control cardiomyocytes (Fig. 2E). The frequency of Ca^{2+} sparks, F/F_0 and full duration at half maximum (FDHM) of Ca^{2+} sparks were increased in S105N Rad TG cardiomyocytes, compared with controls (Fig. 2F), while there were no significant

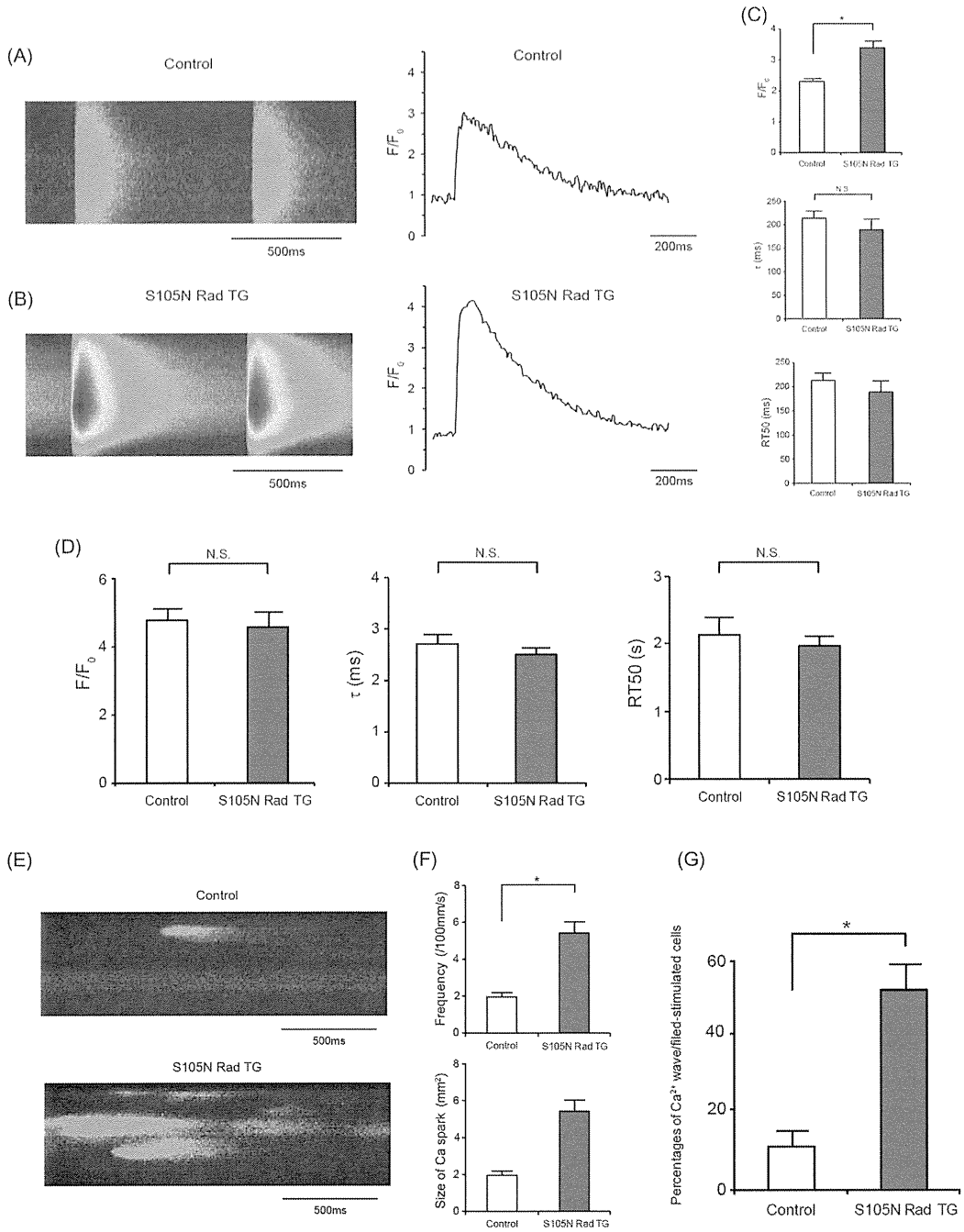

Fig. 2. Intracellular Ca^{2+} imagings of S105N Rad TG mouse and control. The Representative line scan images and their $[Ca^{2+}]_i$ transients by field stimulation at 1 Hz recorded from control (A) and S105N Rad TG cardiomyocytes (B). (C) The parameters of $[Ca^{2+}]_i$ transients (control ($n = 25$) vs S105N Rad TG ($n = 25$), $^*P < 0.05$ vs control). (D) Amplitudes, RT50, and τ of Ca^{2+} transients in response to rapid application of 10 mmol/l caffeine (control ($n = 46$) vs S105N Rad TG ($n = 47$)). (E) Representative traces of Ca^{2+} sparks between control and S105N Rad TG cardiomyocytes. (F) Parameters of Ca^{2+} sparks (control ($n = 30$) vs S105N Rad TG ($n = 32$), $^*P < 0.05$ vs control). The frequency of Ca^{2+} sparks, F/F_0 and full duration at half maximum (FDHM) of Ca^{2+} sparks were increased in S105N Rad TG cardiomyocytes, compared with controls (control ($n = 18$) vs S105N ($n = 24$), $^*P < 0.05$ vs control), while there were no significant differences in full width at half maximum (FWHM). (G) Percentages of spontaneous Ca^{2+} waves in control and S105N Rad TG cardiomyocytes (control ($n = 330$) vs S105N ($n = 315$), $^*P < 0.05$ vs control).

differences in full width at half maximum (FWHM) (Fig. 2F). Notably, spontaneous Ca^{2+} waves were more frequently observed in S105N Rad TG cells than in controls, and there was approximately 3-fold more cardiomyocytes induced with spontaneous Ca^{2+} waves from S105N Rad mice compared to controls (Fig. 2G).

3.3. The phosphorylation of RyR-Ser^{2809} was upregulated in S105N Rad TG mice

To investigate the mechanism behind the increased frequency of the SR Ca^{2+} release channel, the phosphorylation of RyR2 at Serine 2809 (p-RyR2 Ser^{2809}) was examined, with the results showing a significant increase in p-RyR2 Ser^{2809} in S105N Rad TG mice compared with control mice (Fig. 3A).

Furthermore, in order to exclude the non-specific increase in the phosphorylation of RyR2 in genetically S105N Rad TG mouse hearts, we measured the phosphorylation of p-RyR2 Ser^{2809} in S105N Rad-transduced cardiomyocytes using adenoviral vectors. Consistent with *in vivo* mouse experiments, p-RyR2 Ser^{2809} was significantly increased in S105N Rad-transduced cells (Ad S105N Rad cells), compared with cells transduced with control adenovirus (Ad-control cells). In contrast, there was no difference in the saturated level of p-RyR2 Ser^{2809} stimulated with 1 μmol/L isoproterenol (ISO) between them (Fig. 3B). These results indicated that dominant negative suppression of Rad in the heart led to the upregulation of RyR2 activity.

3.4. Rad regulates the PKA signaling pathway

Since the site of Serine 2809 at RyR2 is a phosphorylation point of protein kinase A (PKA) [16,17], we investigated the phosphorylation of PKA. As shown in Fig. 3C, phosphorylated PKA-catalytic subunit at Thr^{197} site (p-PKA-C Thr^{197}) was significantly greater in S105N Rad TG mice, compared with control. Furthermore, PKA kinase assay confirmed the upregulation of p-PKA-C Thr^{197} in S105N Rad TG mice (Fig. 3D).

In order to elucidate the possibility of direct interaction between Rad and PKA, GST pull-down assay was performed. As shown in Fig. 4A, GST WT-Rad interacted with PKA-C, suggesting that the direct interaction of Rad on PKA might lead to the regulation of PKA as well as RyR2 phosphorylation.

There are several upstream molecules of PKA signaling pathway, including β-adrenergic receptors (β-ARs), adenylate cyclase (AC), and cAMP. We measured the concentration of cAMP, protein expression of β1-AR as well as β2-AR from whole hearts, and serum catecholamine. There were no significant differences in the concentration of cAMP and serum catecholamine, as well as expression of β-ARs (Fig. 4B–D).

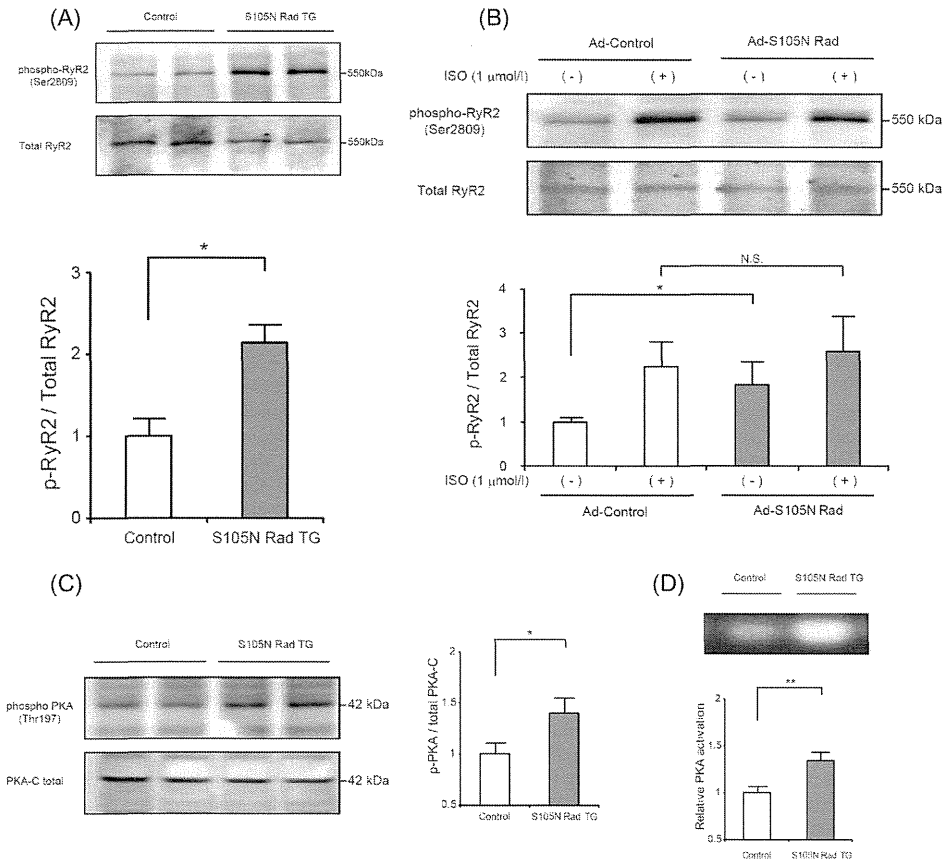

Fig. 3. Phosphorylation of RyR2 and PKA. (A) Western blots of phospho-ryanodine receptor 2 (RyR2) at Ser^{2809} and total RyR2 protein in control and S105N Rad TG mouse hearts. Phosphorylation of RyR2 at Ser^{2809} normalized with total RyR2 protein was significantly enhanced in S105N Rad TG hearts compared with controls ($n = 4$ for both; $^*P < 0.05$ vs control). (B) Western blots of p-RyR2 at Ser^{2809} and total RyR2 protein in isolated adult cardiomyocytes transfected with Ad-GFP or Ad-S105N Rad. The cardiomyocytes overexpressing S105N-Rad showed higher levels of phosphorylation, compared with GFP overexpression alone. Treatment with 1 μM isoproterenol (ISO) abolished the observed change in phosphorylation of Ser^{2809} RyR2 between Ad-GFP and Ad-S105N Rad overexpression (3 independent experiments, $^*P < 0.05$ vs control). (C) Western blots of total PKA (PKA-Total) and phosphorylated PKA catalytic subunit at Thr197 (p-PKA-C Thr^{197}) in S105N-Rad TG hearts and controls (4 independent experiments, $^*P < 0.05$ vs control). (D) PKA kinase assay of total PKA (PKA-Total) and p-PKA-C Thr^{197} in S105N-Rad TG hearts and controls (3 independent experiments, $^*P < 0.05$ vs control).